STATUS OF INDIVIDUAL THESIS

Title of thesis	Remote Sensing and Gravity interpretation of NW Borneo: Integrated Basin Analysis on a GIS platform

I HARRIS SAIFI HAKIMI hereby allow my thesis to be placed at the Information Resources Centre (IRC) of Universiti Teknologi PETRONAS (UTP) with the following conditions:

1. The thesis becomes the property of UTP
2. The IRC of UTP may make copies of the thesis for academic purposes only.
3. This thesis is classified as

☐ Confidential

☑ Non-confidential

Endorsed by

Univerisiti Teknologi Petronas
Bandar Seri Iskandar,
31750 Tronoh, Perak.

Petronas Research Sdn Bhd,
Lot 3288 & Lot 3289,
Off Jalan Ayer Hitam,
Kawasan Insitusi Bangi
43000 Kajang, Selangor.

APPROVAL

UNIVERSITI TEKNOLOGY PETRONAS

Approval by supervisors (s)

The undersigned certify that they have read, and recommend to The Postgraduate Studies Programme for acceptance, a thesis entitled "Remote Sensing and Gravity interpretation of NW Borneo: Integrated Basin Analysis on a GIS platform" submitted by Harris Saifi Hakimi for the fulfilment of the requirements for the degree of Msc Petroleum Geosciences.

Date 29-2-08

Signature :

Supervisor 1 : Dr Mazlan B Hj Madon

Date : 29-2-08

Supervisor 2 : Pn Zakiah Bt Zainol

UNIVERSITI TEKNOLOGI PETRONAS

Remote Sensing and Gravity interpretation of NW Borneo: Integrated Basin Analysis on a GIS platform

By

Harris Saifi Hakimi

A THESIS

SUBMITTED TO THE POSTGRADUATE STUDIES

PROGRAMME

AS A REQUIREMENT FOR THE

DEGREE OF MSC. PETROLEUM GEOSCIENCE

IN PETROLEUM GEOSCIENCE

BANDAR SERI ISKANDAR

PERAK

FEBRUARY, 2008

DECLARATION

I hereby declare that the thesis is based on my original work except for quotations and citations which have been duly acknowledged. I also declare that it has not been previously or currently submitted for any other degree at UTP or other institutions.

Signature: 

Name : HARRIS SAIFI HAKIMI

Date : 20 FEBRUARY, 2008

ACKNOWLEDGEMENT

I would like to express my gratitude and appreciation to the individuals who have made it possible for me to complete this project, which is the final requirement of my pursuit to obtain a Masters in Petroleum Geoscience. Firstly, I would like to thank my supervisors, Dr Mazlan bin Haji Madon and Pn. Zakiah bt Zainol for guidance and teachings they have given to me throughout this project. I would also like to wish many thanks to all the members of the Geoscience family in Petronas Research, especially Ku Rafidah Ku Shafie, Zainol Affendi Abu Bakar, Hasnol Hady bin Ismail and Sarpan b Ishak, for helping and supporting me in many ways during the duration of my project undertaking in Petronas Research. I am truly grateful to the Petronas GIS team, especially Zukhairi Abd Latef who has taught me a lot about the ArcGIS software and helped me to acquire most of the remote sensing data which I have used for this project.

I won't leave out Faishal Abd Rafar from Shell Geomatics, also for teaching me the tricks of ArcGIS, and also En M Idrus b Ismail from Petronas Carigali for helping me acquire the gravity and bathymetry data. I am also grateful towards the lecturers of IFP who taught us the basic knowledge that made it possible for me to construct this project, and also to the Associate Professors and staffs in the department of Postgraduate Studies (Petroleum Geoscience) in UTP for their contributions towards the entire Masters program. Not forgetting all fellow Masters in Petroleum Geoscience students who given me support throughout the project duration. Their encouraging discussions and optimistic ideas made this final hurdle easier for me to endeavour. I wish all of you thank you and good luck for your future undertaking.

Finally, I would like to thank my parents and family for giving me all the encouragement to take up this Masters program, especially to my wife for being patient and understanding while I was completing this project. I dedicate this success to all of you.

ABSTRACT

Geographic Information System (GIS) and remote sensing were applied and used to study the geological evolution of the sedimentary basin of NW Borneo. For this study, Landsat, SRTM, bathymetry and satellite derived gravity data were integrated, manipulated and visualized in a GIS platform by using the capabilities of the GIS software. The onshore region was studied by performing lineament interpretation using Landsat images and SRTM data, whereas in the offshore region bathymetry and gravity data were used to study the lithosphere of the region by gravity modelling.

Lineament interpretation was done by using maps that were generated from the SRTM data (e.g. hillshade and contour maps) viewed concurrently with the Landsat images. Using the GIS tools, gravity and bathymetry data of offshore NW Borneo were extracted to study the lithosphere of this region. The area studied crosses the Dangerous Grounds, Sabah Trough and the Sabah Basin. The lineament trend was interpreted to be evolving from W-E in southwestern Sarawak to NE-SW in the central region onto Sabah, and finally ending in an E-W trend at the northern tip of Sabah. This dynamic change in orientation, coupled with cross-cutting NW-SE lineaments, support the evidence of multiphase tectonic evolution that might result in the series of episodes of subduction and collisions during the geological history of NW Borneo.

For gravity interpretation, the principles of Airy isostasy were used together with the current tectonic model of NW Borneo to model the crust structure to agree. The resulting interpretation shows that the offshore region of NW Borneo is underlain by attenuated crust where the crust is thinnest beneath the Sabah Through.

This thinned crust is buried underneath prograding sediments of the Sabah margin overlying accreationary prism formed during subduction. The thin subducting crust is the remnant of the extended and attenuated continental fragment of Dangerous Grounds.

TABLE OF CONTENTS

LIST OF TABLES

LIST OF FIGURES

CHAPTER 1: INTRODUCTION

1.1 Project Brief

Geographic Information System (GIS) has evolved to become a necessary tool for managing spatial data in the oil and gas industry. Most of the oil and gas companies used GIS as a platform to visualize the spatial data (vector and raster) that are assembled and compiled for the exploration and development (E&P) in an area.

The most important spatial data are the well locations, infrastructures (pipelines/platforms), bathymetry data, coastlines and seismic lines. Remote sensing and topography data are currently being incorporated into the GIS for use in the preliminary assessment of land use, mainly to assist in E&P operations such as seismic acquisition of rig positioning.

However, GIS and remote sensing data in exploration, especially geological studies are is still being under-utilized. These data if integrated could have a huge potential in studying the geological evolution of sedimentary basins. This study is aimed at integrating the various geological data, including remote sensing images into a GIS platform to study the structure or tectonic evolution of a basin for future petroleum exploration.

1.2 Objectives

The objectives of this study is to a) integrated the various datasets (i.e. remote sensing, gravity, bathymetry/topography) into the GIS, b) to interpret the lineaments corresponding to the remote sensing data and c) to perform gravity modelling on parts of the study area.

The area chosen for the study is Northwest Borneo which represents a typical setting for a foreland basin.

1.3 Scope of Investigation

1.3.1 General

The data integrated on to the GIS platform comprises remote sensing data, such as Landsat images and Shuttle Radar Topographic Mission (SRTM) images for the onshore regions, and bathymetry data and satellite derived free air gravity data for the offshore regions. From the data sets, lineament interpretations are done visually on ArcGIS software where the use of the remote sensing data and topography/bathymetry data are viewed concurrently.

The satellite derived gravity data will be used for gravity to study the basin evolution of the study area. A profile was selected from the dataset, and gravity modelling was attempted on that profile. The focus of the gravity study is the offshore regions of the study area.

1.3.2 Specifics

a) Integration of various data sets of the study area into a GIS platform. The data sets used for this study are: -

   i. Remote sensing
      - Landsat 7 (ETM+) data of NW Borneo
      - Shuttle Radar Topographic Mission (SRTM) 3 data

   ii. Satellite gravity data from Geodetic Missions of GEOSAT and ERS-1 satellites, compiled and processed by GETECH.

   iii. Bathymetry data acquired from GEBCO Digital Atlas (GDA)

b) Interpretation of the basin evolution of the study area using the various data sets available. This includes lineament interpretation of the study area.

c) Create a gravity model (profile) from the results of the interpretation.

1.4 Software

As mentioned in the objectives, this study can be divided into two main parts. One involves a structural study of the study area using data compiled into a GIS and the other is using the structural data to perform gravity modelling. Below is the list of software used: -

a) ArcMap 9.2

ArcMap 9.2 is one of the main software products that forms a part of the ArcGIS 9 integrated GIS package. This software was mainly used for spatial data compilation, visualization and interpretation. Its 3D Analyst extension was used to create 3D surfaces.

b) GM-Sys

GM-Sys is a program for calculating the gravity and magnetic response from a geological model (GM-Sys User's Guide version 4.9). This software was used to model a structural profile from exported from the GIS from the observed gravity data.

CHAPTER 2: LITERATURE REVIEW

2.1 Study Area

2.1.1 Introduction

The island of Borneo (Figures 2.1, 2.2) is located to the south of the South China Basin, and sits partly on the eastern portion of the Sunda Shelf. The states of Sabah and Sarawak occupy the North West regions of Borneo (Figure 2.2).

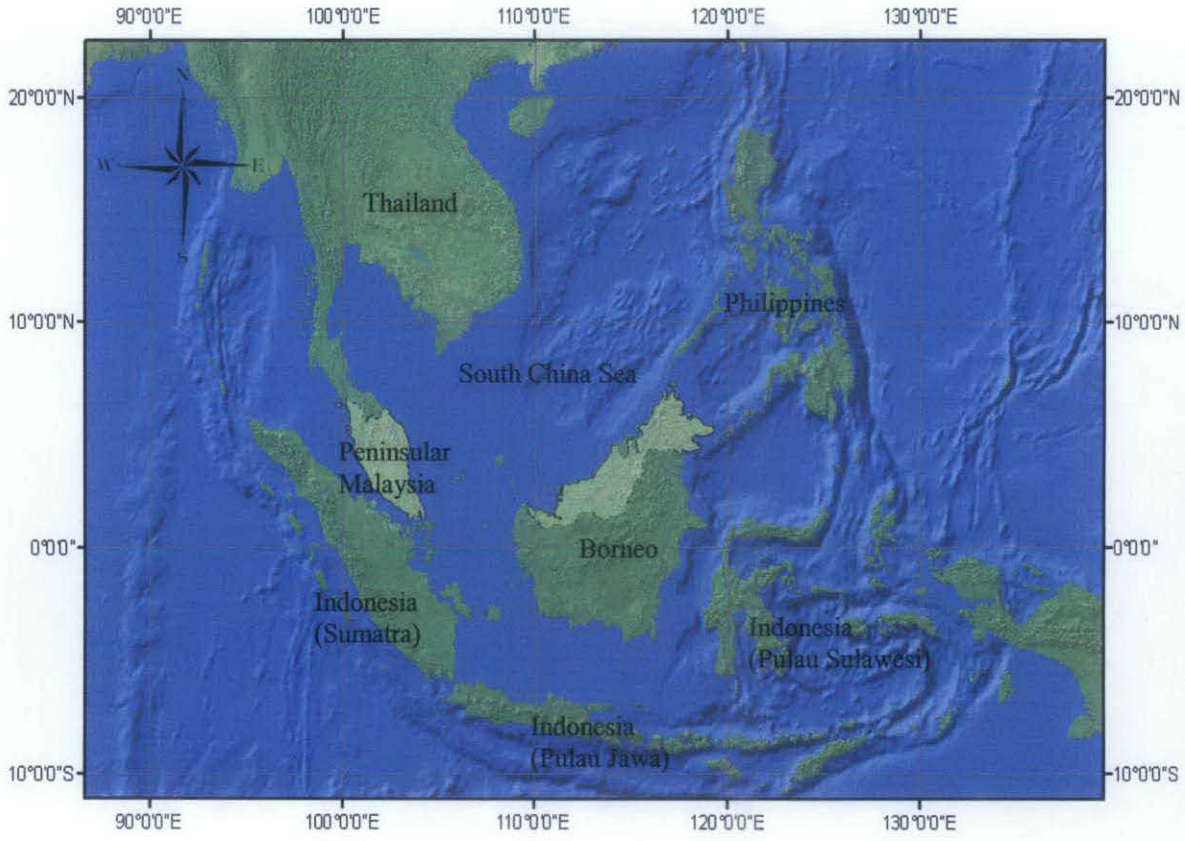

Figure 2.1: Location map of the island of Borneo in South East Asia

The geological history of NW Borneo has been extensively studied over the decades by many (i.e. Hazebroek and Tan, 1993; Mazlan Madon, 1999c; Hutchison, 2004). Its tectonic evolution has been strongly related to the events leading up to the opening of the South China Sea (Taylor and Hayes, 1980; Hall, 1996; Mazlan Madon, 1999a). Hence, the evolution of the South China Sea has a major impact on the structural evolution of Sabah and Sarawak (Mazlan Madon, 1999a).

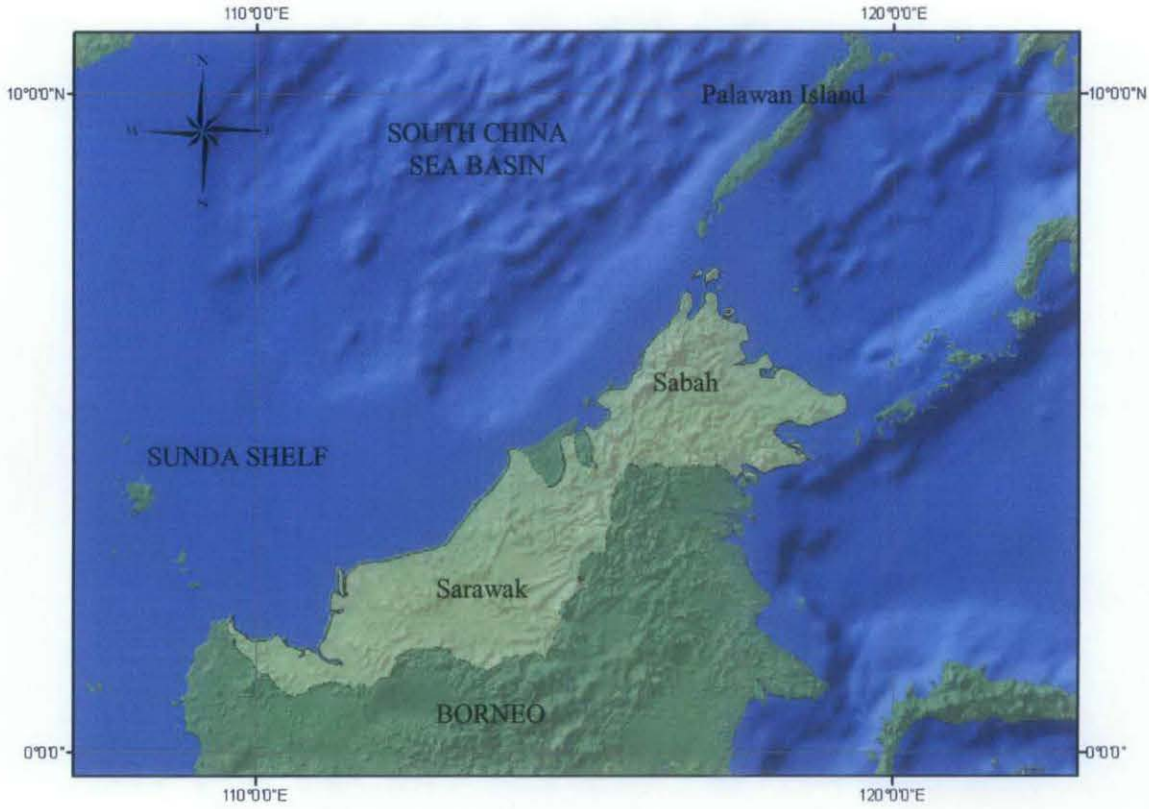

Figure 2.2: Location of Sabah and Sarawak in North West Borneo, which is located south of the South China Sea Basin, and east of the Sunda Shelf

2.1.2 History of the Tectonic Evolution of South China Sea

Much of the tectonic history of NW Borneo revolves with the tectonic evolution that led to the opening up of the South China Sea (SCS) (Figure 2.1). The SCS originated from a passive rifting, pull-apart and breakup of the South China continent (Taylor and Hayes, 1980; Hayes and Nissen, 2005). From Late Cretaceous to Middle Miocene, the South China continent started to stretch in an approximately N-S direction to create a passive rifting at the margins and crustal thinning at the extinct ridge (Wang et al., 2006).

By Oligocene, the sea-floor spreading in the South China Sea caused several micro-continental blocks such as Reed Bank, Dangerous Grounds, and Luconia Block to drift southwards and collide with the northern Borneo margin (Holloway, 1981). These rifted micro-continental block drifted southwards and collided with Borneo.

This collision has caused an oceanic basin that once separated the blocks with Borneo to be subducted beneath the Borneo margin (Taylor and Hayes, 1980) and caused the uplift of the Rajang and Crocker (Rajang Group Fold-Thrust Belt) (Figure 2.3, 2.5) orogeny that extends from the south west of Sarawak through the north to Sabah (James, 1984; Hazebroek and Tan, 1993; Hazebroek et al., 1994). This "remnant ocean" (Figure 2.3, 2.4) was described as the proto South China Sea (also referred as the Rajang Sea) that once separated the drifted continental blocks (i.e. Luconia, Dangerous Grounds) from Borneo.

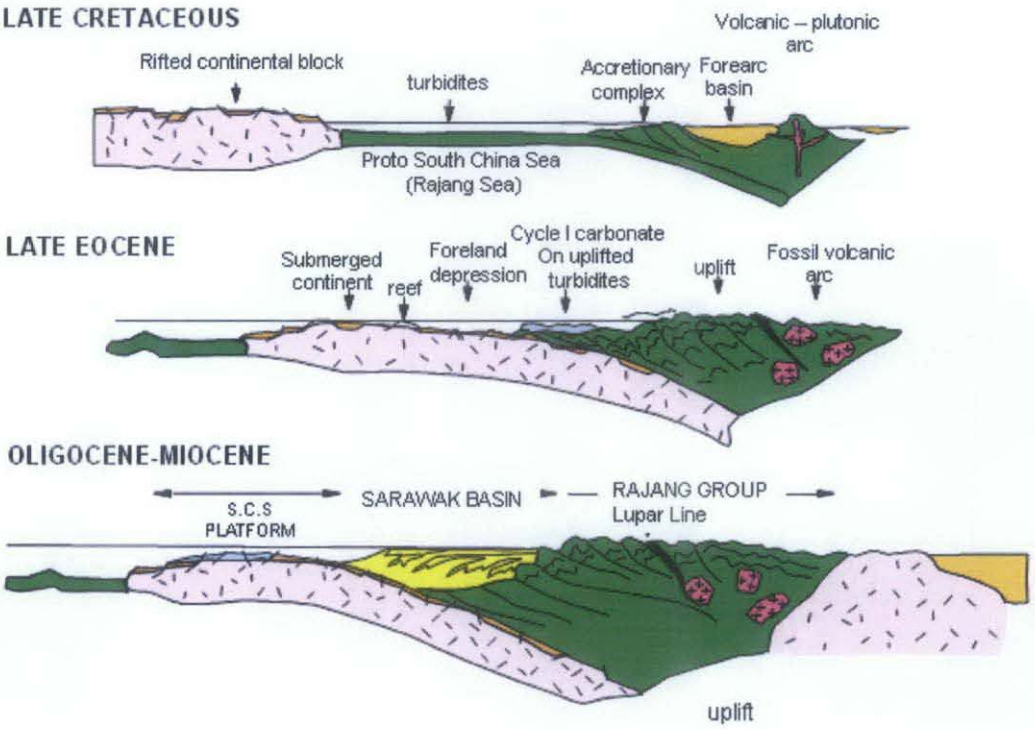

Figure 2.3: A schematic illustration of the tectonic evolution of NW Borneo, beginning with the subduction of the Proto South China and formation of an accretionary complex (Rajang Group) till the collision of NW Borneo with a rifted continental block (Luconia Block) (After Mazlan Madon, 1999c).

The sea-floor spreading of the South China Sea which caused the rifted continents to collide with Borneo was believed to have been oriented north-south and subsequently was reorganized to northwest-southeastwards until late Miocene (Taylor and Hayes, 1983; Briais et al., 1993; Pubellier et al., 2003). This could be related to the oblique orientation closure/trench pull during the subduction of the Rajang Sea/proto South China Sea (Mazlan Madon, 1999b; Pubellier et al., 2003)

The rifting and collision of the mentioned continental blocks (i.e. Luconia, Dangerous Grounds) from the north and its resulting closure of the Rajang Sea were said to be diachronous. The timing of the collision between Luconia Block and Sarawak margin occurred first (during Late Eocene) and followed by Dangerous Grounds (during Early Miocene) (Hutchison, 1996, 2004; Holloway, 1981).

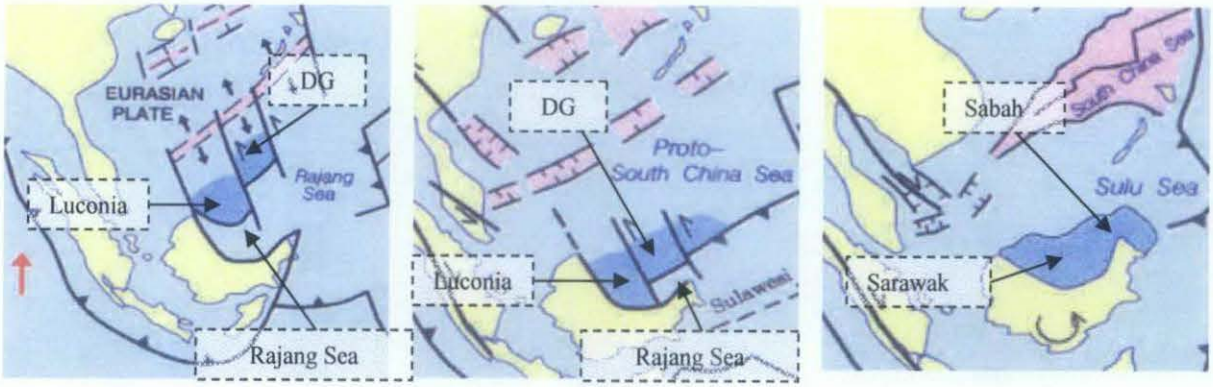

Figure 2.4: A schematic illustration of the reconstruction of the tectonic evolution of South China Sea (modified after Hall, 1996).

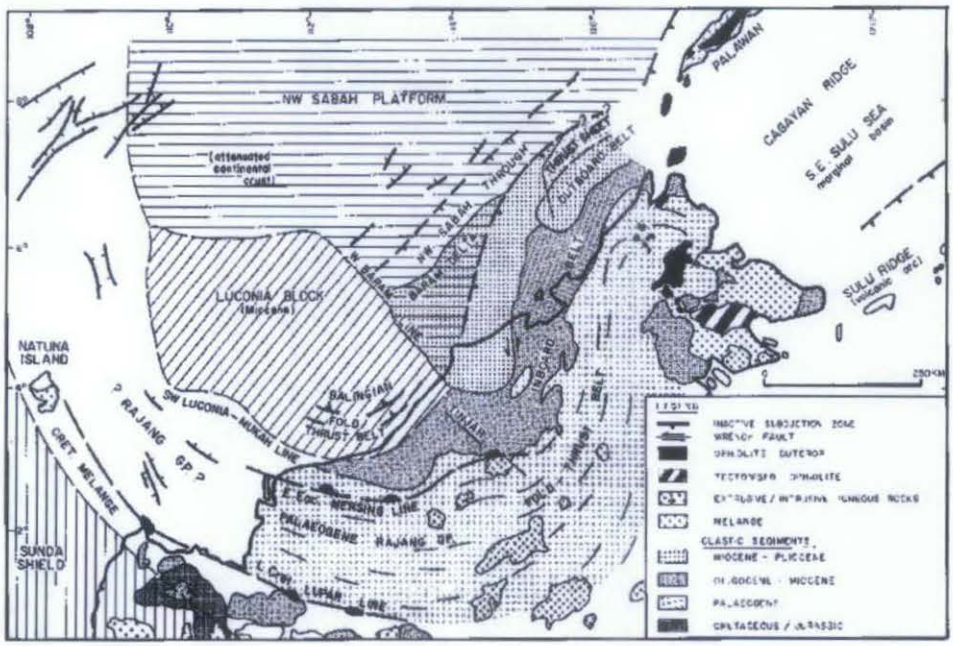

Figure 2.5: A map showing the regional geology of NW Borneo (after Hazebroek and Tan, 1993)

2.1.3 Luconia Block

The Luconia Block (Figure 2.4 and 2.5) is one of a series of continental fragments that rifted off and drifted from southern China during Late Cretaceous to Eocene (Holloway, 1981; James 1984) and collided with Borneo. Its rifting and drifting phase has been interpreted as also parallel to the NW Sabah Platform, together with North Palawan Block, Reed Bank and Dangerous Grounds (Holloway, 1981). Taylor and Hayes (1980) described the Luconia block as to have been incorporated into the Sunda Shelf (Figure 2.5) by sediments prograded out into it. The Luconia Block also is observed to be the termination point of the NW Sabah Trough (Hazebroek and Tan, 1993).

The Luconia Block has subsided and is buried with more than 12 km of sediments overlying it (Mazlan Madon, 1999c). It is also characterized by a large number of carbonate reef buildups (Scherer, 1980). The continental slope transiting from the Sunda Shelf to the Dangerous Grounds is characterized by a narrow transition zone of slightly steeper slope and the continental slope is generally unfaulted and draped by younger sediments (Hutchison, 2004).

Thinning of the continental crust prior to rifting at the southern China margin is one explanation for the subsidence of the Luconia Block (Mazlan Madon, 1999b). The larger subsidence is a result of the flexural loading of the South China Sea lithosphere by the Rajang Group orogen during the late Eocene times.

2.1.4 Rajang Group Fold-Thrust Belt

The previous section briefly explains a continental fragment, the Luconia Block which rifted and drifted from the Southern China in the Late Cretaceous to Eocene collided with the West Borneo Basement and subducted under it (James, 1984; Hazebroek and Tan, 1993; Hazebroek et al., 1994). It is interpreted that a subduction zone lies along the northern margin of West Borneo Basement where the drifted Luconia Block subducted under it, and is now underlying the Sarawak continental shelf north to this subduction zone (Taylor and Hayes, 1980, Hutchison, 1996).

The collision which resulted in the closure of the Rajang Sea in the Late Eocene that once separated Luconia and West Borneo, and also the deformation and uplift of the Rajang Group to form the Rajang Fold-Thrust-Belt was interpreted as the resulting accretionary prism that sutured from the collision process (James, 1984; Hazebroek and Tan, 1993; Hutchison, 1996; Mazlan Madon, 1999b). Deepwater turbiditic sediments (flysch) of the Rajang-Fold-Thrust Belt are evidence of a subducted oceanic lithosphere prior to the collision (Mazlan Madon, 1999a).

After the Rajang Sea closed during the Late Eocene, the Sarawak margin began to form as a foreland basin which is known as the Sarawak Basin. Coastal progradation northwards from the uplifted Rajang Fold-Thrust Belt provided the sediment supply to which gradually filled the Sarawak Basin and evolved into a passive margin (Mazlan Madon, 1999c).

In western Sabah, the collision of Dangerous Grounds-Reed Bank and Sabah was the second collision after the Sarawak-Luconia, and was termed as the Sabah Orogeny (Hutchison, 1996). This resulted in the uplift of the deepwater Crocker Formation.

2.1.5 NW Sabah Platform

The NW Sabah Platform (Figure 2.5) is a part of the South China Sea Basin and is interpreted to consist of attenuated continental crust (Hazebroek and Tan, 1993). The NW Sabah Platform includes the Dangerous Grounds, Reed Bank, and Northern Palawan and it is characterized by half-graben and tilted fault blocks infilled by sediments (Schluter et al., 1996; Mazlan Madon, 1999b; Mazlan Madon et al., 1999).

Hutchison (2004) explained the Dangerous Grounds as lying between the sea-floor spreading and the Sunda continental shelf. It is a 170-330 km wide zone composed of strongly attenuated continental crust with the oldest post-rift draping strata having an age of early Middle Miocene (~16 Ma) lying over a breakup unconformity known as the Middle Miocene Unconformity (MMU) (Hutchison, 2004).

The province is also characterized by normal faulting in the form of half grabens. Overlying the grabens are pre-rift to early rift sequences and syn-rift sequences, and the post-rift sequences drapes over the underlying rift sequences (Hutchison, 2004). Hutchison (2004) also mentioned that the subsidence of the Dangerous Ground is due to isostatic adjustments following crustal attenuation and the break-up MMU causing the bathyal strata to drape over the syn-rift sequence. The age of these younger sequences is from Middle Miocene to Recent (Hutchison, 2004).

2.1.6 NW Sabah Trough

The NW Sabah Trough (Figures 2.5, 2.6) is also known as the NW Borneo Trough, Palawan Trough or Nansha Trough. It divides the Sabah continental slope from the Dangerous Grounds (Mazlan Madon, 1999c). The occurrence of this deep and narrow trough and its adjacent anticlines has resulted in a number of interpretations from previous workers.

One of the earliest interpretations is that the trough was once a subduction trench and the anticlines as its consequential accreational prism that was formed by south-eastward subduction of the mentioned proto-South China Sea (Haile, 1973; Hamilton, 1979). According to Hutchison (2004), it may also be regarded as a foredeep, resulting from a continental lithosphere descending beneath the collision zone.

Another interpretation suggested that it was a back-arc rift basin which had undergone elastic down-warping of thinned crust in response to the gravity load (Hinz and Schluter, 1985; Hinz et al., 1989; Hazebroek and Tan, 1993; Schluter et al., 1996). The later models portrayed the anticlines as a backthrust product of the southward subduction of NW Sulu Sea (Hinz and Schluter, 1985; Schluter et al., 1996) or a product of gravity slump (Hazebroek and Tan, 1993).

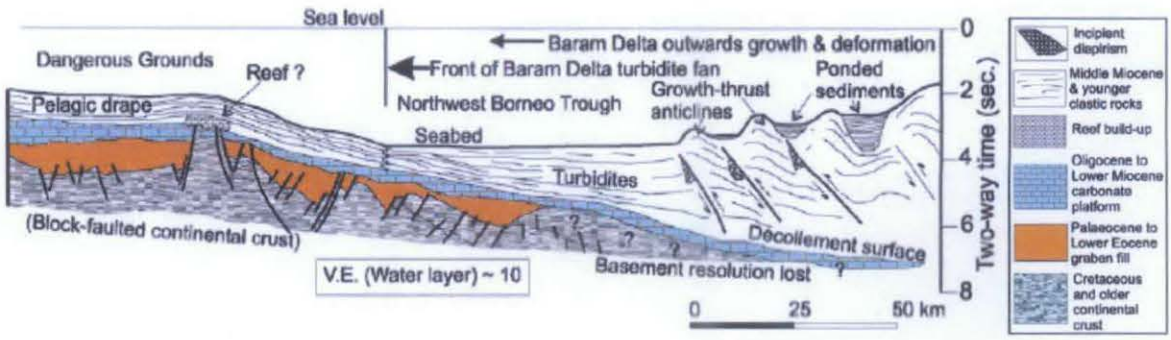

Figure 2.6: A geological interpretation profile across the Palawan Slope, NW Sabah Trough, and Dangerous Grounds (after Hutchinson, 1996).

The adjacent anticlinal features of the NW Sabah Trough (Figure 2.6) are tightly folded anticlines and are called the Baram Delta Toe Zone (i.e. Hazebroek and Tan, 1993; Hutchison, 2004), Palawan-Borneo Nappe (i.e. Yan and Liu, 2004) or Palawan Slope (Figure 1.8). Hazebroek and Tan (1993) attributed that this province as resulted from typical delta tectonics that could also be divided into a proximal part and a distal part. The proximal part was dominated by extensional growth-faulting, and the distal part as being dominated by overthrust anticlines representing toe-thrust zone of the delta.

The Baram Delta toe zone causes the turbiditic currents to flow into the adjacent synclines including the Sabah Trough (Grant, 2003; Hutchison, 2004). Recent studies by Yan and Liu (2004) observed 7-8km of sediments in the upthrust area. The sediments that fill the so-called trench were mapped as thick sandy turbidites of Oligocene to Lower Miocene age with western Borneo being the source area (Hutchison, 2004).

2.2 Remote sensing

2.2.1 Introduction

In general, remote sensing means obtaining information on an object without being in contact with the object itself. Remote sensing mainly involves two sciences which

is acquiring the data of an object from a distal observation device (sensor), and interpreting the physical attributes of the object (Gupta, 2003).

In the field of satellite imagery, remote sensing refers to detecting the electromagnetic energy emitted or reflected from an object, and in this case the earth. The wavelength utilized in the study range from the electromagnetic spectrum then can be used to differentiate various types of objects, typically dry soil, wet soil, vegetation, etc.

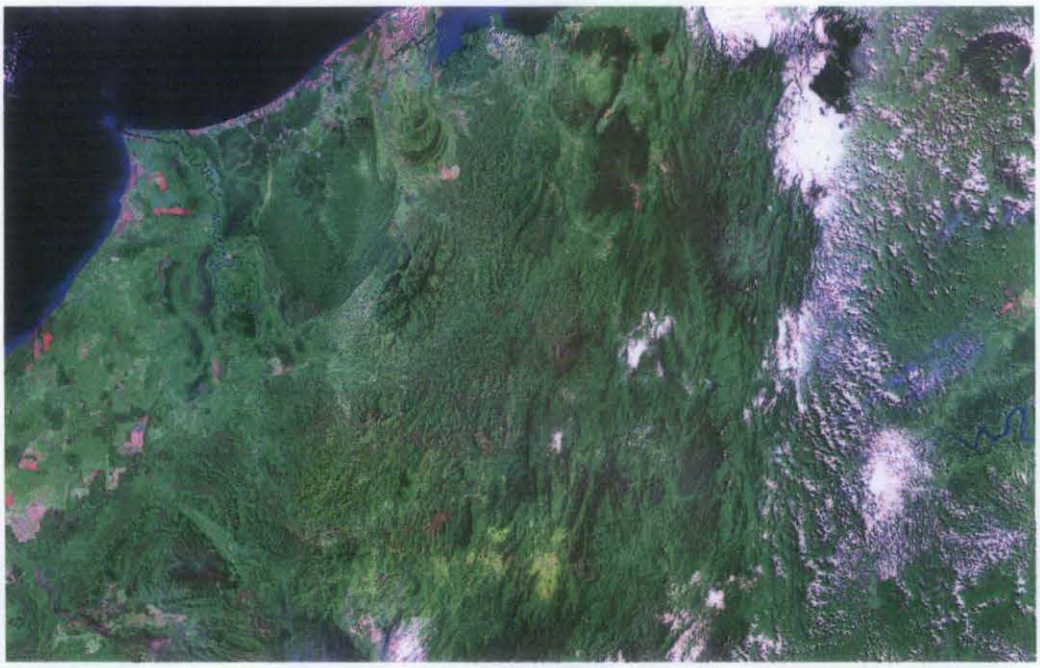

Figure 2.7: A Landsat 7 ETM+ scene of NW Borneo displayed in Band 7-4-2

2.2.2 Application

Remote sensing studies have been widely applied in various branches of geology such as geomorphology, structural and lithological mapping, mineral and oil exploration, etc. The main advantage of using satellite imagery is the large extend of data coverage and its ability to cover areas that may not be accessible for ground survey.

Remote sensing techniques have been used to supplement and integrate structural field data as well as providing a new dimension of synoptic view. Walker (2006)

used satellite imagery and digital topography to asses the potential for active strike-slip and thrust faulting in the Kerman province in South East Iran. He used light coloured exposed marl deposits within the core of the folds detected from the satellite images to identify anticlinal fault-related folding. Active folding was also detected by the presence of uplifted and incised gravel surfaces within anticlines, and sometimes by the diversion of drainage networks.

Raharimahefa and Kusky (2006) used Landsat ETM+ imagery and SAR data complemented with fieldwork to study the structural framework of the southern Betsimisaraka Suture in Madagascar. The remote sensing studies conducted in Madagascar are very useful because many areas of the island were inaccessible.

Studies on the structural and regional tectonic on remote sensing images are commonly conducted by detecting lineaments and analyzing them. It has since become an effective approach to understand tectonic origins. Lineaments can be mapped from all kinds of remote sensing images.

2.3 Lineaments

2.3.1 Definition

Lineaments are defined as more or less rectilinear alignment features that can be seen on satellite images, aerial photographs and digital elevation models (DEM) (Gupta, 2003). They form one of the most obvious features on high altitude aerial or space images and hence the term has been applied for different geological features such as shear zones/faults, rift valleys, truncation of outcrops, fold axial trace, joints and fracture traces, fissures, lithological layering, stream and valleys, vegetation linear, topographic alignments and others (Gupta, 2003).

Over the years, lineament mapping from remote sensed images has been widely used due to its ability to perform regional scale studies that significantly saves cost and time as compared to field mapping. Lineament interpretations were also verified by field observations to build an estimate of confidence level.

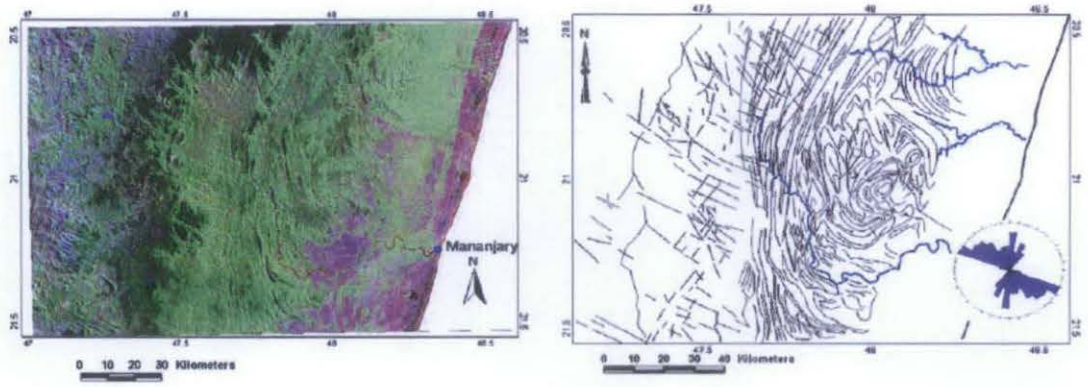

a) b)

Figure 2.8: a) Landsat image of the Mananjary-Vohilava region, Madagascar. b) Lineaments produced from a) (After Raharimahefa and Kusty, 2006)

Lineaments can be mapped from all types of remote sensing images. Generally, lineaments would occur as straight, curvilinear, parallel or en-echelon features. Lineaments can also be mapped on simple data products or on processed/enhanced images such as digital enhancing techniques or special filters (Gupta, 2003).

However, lineaments are not the only result of tectonic expressions. Lithological contacts, intersection of bedding and topography, some wind erosion and glacial features could also appear as lineaments in images. Artefacts are also common in enhanced images and could render interpretation (Gupta, 2003). Therefore, it is important to be able to discriminate the lineaments related to tectonic effects, and the non-tectonic related lineaments.

2.3.2 Lineament Interpretation/Extraction

Lineaments can be extracted through the means of visual interpretation and manual hand tracing methods using tone, colour, texture, pattern, etc. Alternatively, lineaments can also be extracted automatically using program algorithms. Koike et al., 1995 carried out auto-detection of lineament that was based on the segment tracing algorithm (STA) technique on topographic and panchromatic ETM+ images.

Automatic lineament extraction methods however are blind because they cannot discriminate between tectonic and non-tectonic lineament features, but they can extract the general structural trend of a study area faster without interpretation bias

(Abarca, 2006). Automatic lineament extraction methods may lead to the detection of many artefacts or non-geological related lineaments due to illumination, shadows, etc, in the remote sensing image. As such, the visual interpretation technique is generally preferred and extensively applied (Gupta, 2003).

Lineaments on remote sensing images or Digital Elevation/Terrain Models (DEM/DTM) can also be enhanced by certain processing or enhancing algorithms to make them easier for detection and interpretation. Differing band ratio combinations can be used to shadow relief and enhance the effects of topography. Solomon and Ghebreap (2006) used Landsat TM images with Red-Green-Blue (RGB) colour combinations of 5-4-1 bands for visual interpretation of lineaments in the highlands of Eritrea. They also integrated Principal Component Analysis (PCA) to reduce spectral redundancy and enhance lineaments.

Raharimahefa and Kusky (2006) used a combination of Landsat -7 and -4 bands and Synthetic Aperture Radar L-band for structural mapping. Analytical hill shading technique was applied to DEM and used by Masoud and Koike (2006) to generate shaded topographic images that eased lineament detection and extraction. Solomon (2003) also used directional filters to highlight linear features in their respective direction.

2.3.3 Lineament Application

Lineament studies have been applied in various fields such as mineral exploration, petroleum prospecting, groundwater investigation and others. Lineament studies have been conducted to investigate regional tectonic studies, fractured and deformation structural patterns, delineation of major structural units, drainage patterns, and others.

In 2006, Masoud and Koike used lineaments analysis to understand the development of depression zones, factures and faults in the Siwa region, Egypt. The interpretation of the lineaments to the tectonic domain provided new insights in the regional tectonic framework and evolution near the northern boundary of the Africa plate.

The structural interpretation carried out on remote sensing images was consistent with other structural models from previous studies.

Another example on the studying of surface expressions of geological structures such as fractures (faults and joints), shear zones, foliations, structural discontinuities of rocks and other features related to tectonic activity from lineament analysis is that by Solomon and Ghebreab in 2006. In this study, lineament analyses from Landsat TM images over the highlands of Eritrea were characterized to understand its tectonic origin and relationship to the rift tectonics of the Red Sea/Danakil.

Solomon (2003) studied lineaments from remote sensing images and digital elevation models to prepare drainage maps for the assessment of groundwater potential in Eritrea. He concluded that areas with a high density of lineaments are favourable sites for groundwater exploration.

2.4 Shuttle Radar Topographic Mission (SRTM)

2.4.1 Introduction

In February 2000, the Shuttle Radar Topography Mission (SRTM) was jointly launched by NASA, the National Geospatial-Intelligence Agency, and the German and Italian Space Agency. The objective of the SRTM project was to provide a complete high resolution digital elevation model of the Earth. It uses a dual radar antenna system to acquire interferometric radar data. SRTM releases data at two horizontal resolutions; 1 arc-second by 1 arc-second (approximately 30m by 30m) covering the United States, and 3 arc seconds (approximately 90 meters) for global coverage (Rodriguez et al., 2005).

SRTM uses the principle of interferometry where 2 radar antennas with a range difference between them are mounted on a moving platform. Therefore both the antennas will image the surface from its different respective points. The SRTM acquired C-band and X-band where the look angles were 30-60 degrees and 50-55 degrees respectively (Gupta, 2003).

2.4.2 Application

The DEMs generated by SRTM have very high resolution and can reach a height resolution of 10m for C-band and 6m for X-band. DEM data are a very useful input for depicting surfaces or topography and is applied in many geological studies (Gupta, 2003). Modern geosciences have a need for practical, reliable and high quality global digital elevation models (DEM) as a source for topographic information. As studies and the regional understanding of geology are increasingly being conducted on a global scale, topographic spatial data are now used due to their extensive and wide coverage. SRTM data has become a very popular and reliable source for DEMs (Rodriguez et al., 2005).

2.5 Geographic Information System (GIS)

2.5.1 Introduction

Gupta (2003) defines Geographic Information System (GIS) as a higher-order computer-based system which permits storage, manipulation, display and output of spatial information. GIS technology has evolved to be useful for the integration of various spatial data from different disciplines.

2.5.2 GIS applications in Geological Studies

Remote sensing data has become an important data input for GIS studies. Solomon (2003) integrated remote sensing data with other spatial data into a GIS to study the groundwater potential in Eritrea. Grohmann et al (2006) used GIS to perform analyses including slope and aspect calculations in their study. Structural studies have also been conducted on GIS platforms. Pubellier et al. (2003) integrated kinematics parameters from GPS observations into a GIS to reconstruct pericratonic mountain ranges of South East Asia.

GIS has become an important platform for data integration and analysis because of its flexibility in integrating different types of data and in displaying all the data in a concurrent display and hence its ability to run numerous operations and analysis.

2.6 Satellite Gravity

2.6.1 Basics of satellite gravity

Satellite gravity-derived data relies on the fact that the shape of the sea-surface is dependent on the gravity field or the surface of the ocean is an "equipotential surface" of the earth's gravity field (Sandwell and Smith, 2006). This equipotential ocean surface is more nearly matched by an ellipsoid (instead of a sphere) of revolution where the polar diameter is less than the equatorial diameter. The ocean surface heights however have differences because they are affected by minute variations in the earth's gravitational field (GETECH, 2007; Sandwell and Smith, 2006).

These differences can be described as tiny bumps and dips in the ocean's surface. These tiny bumps and dips in the geoidal height can be measured using an accurate radar mounted on a satellite (satellite altimeters). One such example is the Geosat satellite which was launched by the US Navy in 1985 to map the geoid height (Sandwell and Smith, 2006).

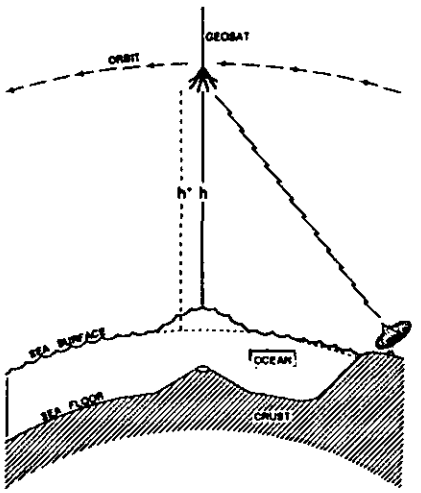

Figure 2.9: A pulse-limited radar altimeter orbits at an altitude of about 800 km and measures the distance to the closest ocean surface by recording the travel time pulse (after Sandwell and Smith, 1997)

These satellite altimeters measure the range of the sea surface from the satellite using reflected radar pulses from the sea surface, and converting this range which is

measured in time, to distance after applying corrections for atmospheric effects. The heights of these satellites above the ellipsoid h^* are measured by tracking the satellites from a globally-distributed network of lasers and/or Doppler stations (Sandwell and Smith, 2006).

By comparing this distance with the altitude of satellites above the ellipsoid (from ephemeris/orbit information), the difference of these two values gives the sea surface height (SSH). This sea surface height, after correction for transient variations such as tides, represents the equipotential surface of the earth's gravity field. (Sandwell and Smith, 1997; Sandwell and Smith, 2006; GETECH, 2007).

The Geosat satellite can measure a horizontal resolution of 10-15 km (6 - 10 minutes) with a vertical resolution of 0.03 m (Sandwell and Smith, 2006). In terms of accuracy, when compared with gravity data acquired on shipboard, the accuracy of the satellite derived gravity anomaly is about 4-7 mGal for random ship tracks and improves to 3 mGal when the ship track follows a Geosat Exact Repeat Mission track line (Sandwell and Smith, 1997).

2.6.2 ERS1 and GEOSAT Geodetic Missions

Satellite gravity or satellite altimeter data from the ERS1 and GEOSAT Geodetic Missions have been used in the evaluation of the Earth gravity field. It has been used as one of the most important data sets for marine gravity evaluation because it is dense, efficient and practical, considering the coverage of the data and the ability to acquire data in remote areas.

The GEOSAT Geodetic Mission was carried out over eighteen months from 1985 to 1986 along an average track spacing of 5km at the equator. The data acquired was de-classified by the US government in September 1995. The ERS-1 Geodetic Mission was carried out by the European Space Agency along an average track of 8km at the equator. Altimetry from the ERS-1 geodetic mission yields a coverage that is ten times denser than that of the ERS-1 35-day repeat mission and around 36 times better than that of the TOPEX/POSEIDON mission (Knudsen and Andersen, 1997; GETECH, 2007).

The Geodetic Mission of GEOSAT is roughly 1.5 times the geodetic mission of ERS-1 and the track spacing between the ground tracks should theoretically be improved by a factor of 1.5 as compared with the track spacing of ERS-1. This combined use of altimetry from the ERS-1 and GEOSAT geodetic mission resulted in a gravity field that has been mapped world wide with a resolution of 3'45" by 3'45" (Andersen and Knudsen, 1997).

2.7 Gravity interpretation

2.7.1 Introduction

Gravity anomalies are a result of horizontal variations or discontinuities at any depths below the surface. The objective of gravity interpretation is to deduce the geological character of the subsurface from the variations of the gravity field observed (Nettleton, 1971). However the limitation of gravity interpretation is that it is completely ambiguous.

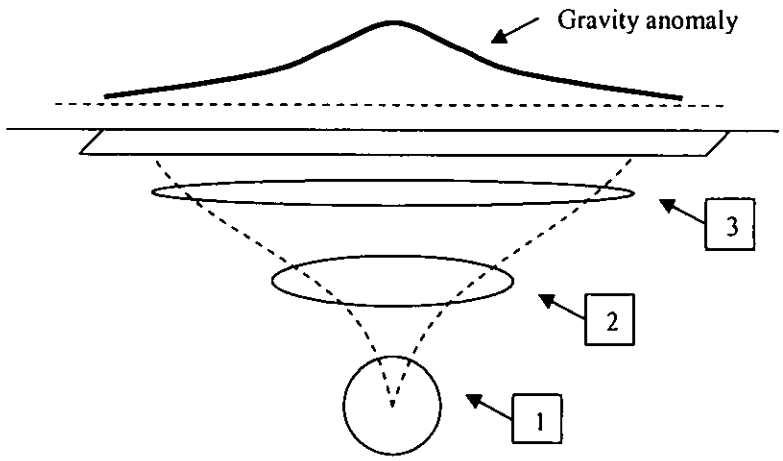

Figure 2.10: "Cone of Sources"; 1, 2 and 3 are bodies with similar mass anomaly where all can be accounted for the same gravity anomaly. 2 and 3 are shallower and broader bodies respectively as compared to 1 (Modified after Nettleton, 1971).

The gravity signature observed can be accounted for several different models of the earth structure as a "cone of sources" explained by Nettleton (1971) (Figure 2.10). Therefore, there is no unique way to determine the depth and form of density

variations that are causing the gravity anomaly just by control of the gravity field alone.

However by using other available sources of geological information such as depths of major density contrast which are obtainable from drillings or other geophysical observations (magnetics, seismic), estimates of depths to possible density contrast (e.g. depth to Mohorovicic Discontinuity), estimates of probable lithology, or general geological reasoning could eventually constrain and limit the possibilities and theoretical ambiguities hence making gravity interpretation useful for geological investigations.

2.7.2 Previous gravity studies on study area

Milsom et al. (1997) interpreted satellite-derived free air gravity data from offshore NW Sabah to investigate the occurrence of a strong gravity low related to the presence of the Sabah Trough. This gravity low is bounded by the gravity highs of Baram Delta, which is located southeast of the trough and the Spratly Rise (Dangerous Grounds), northwest from the trough. They attributed this free air gravity pattern as conforming to a foreland basin model.

By assigning densities for the crust and the materials overlying and underlying the crust, and also by assuming an initial crust thickness, they were able to produce a computed gravity profile across the area. In their findings, it was observed that the computed and observed gravity profiles can be matched if only there is a thinner crust beneath the area.

They concluded that the crustal thinning beneath the area is a result of crustal attenuation of an extended margin that had rifted from Eurasia and had subsided beneath NW Borneo. This extended continental margin is the Spratly Rise.

2.7.3 The concept of isostasy

Isostasy is a term that would describe how gravitational equilibrium exists within the earth's lithosphere and asthenosphere, whereby the lighter crust is floating on the underlying denser mantle and how these properties supports the occurrence of topography. The development of the concept has led to the discovery of two leading theories (Nettleton, 1971; Watts, 2001):

a) Pratt theory – Assumes that the density of the earth's material below sea level and under areas of high topography is lower than the average and that the low density material extends to a fixed "depth of compensation".

b) Airy theory – Assumes that there is a discontinuity in density at some depth within the earth's crust and that this discontinuity is at variable depths, being deeper under high topography and shallower under low topography.

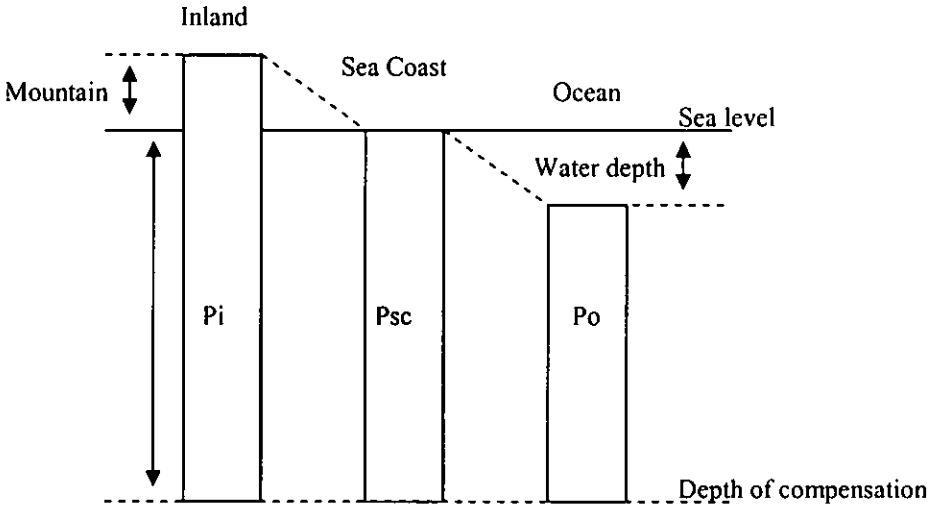

Figure 2.11: Pratt's model of isostasy where *Pi* is the density of the crust beneath a mountain, *Psc* the density of the crust beneath the sea coast and *Po*, the density of the crust beneath the oceans and *Pi* < *Psc* < *Po*. The depth of compensation is fixed. (Modified after Watts, 2001)

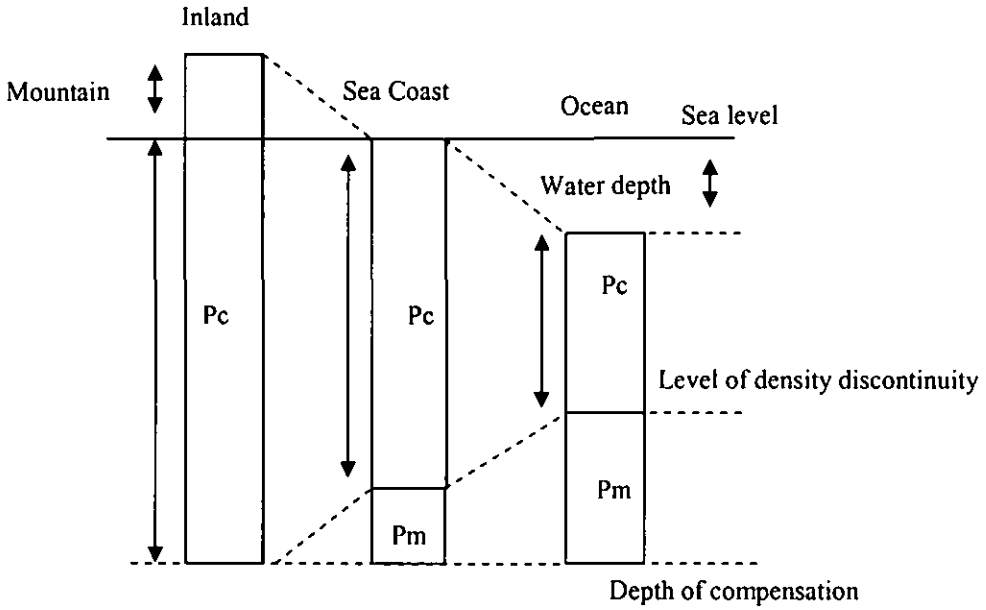

Figure 2.12: Airy's model of isostasy where *Pc* is the density of the crust and is the same everywhere at every depth. *Pm* is the density of the mantle and is the same every where at any depth, and *Pc* < *Pm*. The level of the discontinuity of density is at various depths, being deeper beneath mountains and shallower beneath ocean basins (Modified after Watts, 2001).

CHAPTER 3: DATASETS

3.1 Satellite Derived Gravity Data

3.1.1 GETECH Global Gravity Database

The offshore gravity data for the study area of NW Borneo was taken from GETECH's South East Asia Satellite Gravity Study, 1998. The data constitutes a part of the Global Gravity Database which has been compiled for Petronas by GETECH in 2007. This database consist of the satellite-derived Global Continental margins Gravity Study (GCMGS), GETECH's onshore continental gravity compilations, public domain compilation data sets and public domain geopotential model of the EGM96.

The gravity field products are derived from satellite altimeter data recorded by the complete Geodetic Missions of GEOSAT and ERS-1 satellites. GETECH processed the data using a combination of GETECH's processing technology and techniques to produce a satellite gravity dataset with a resolution down to 0.02 degrees (approx. 2km) rendering it more reliable and with fewer artefacts (GETECH, 2007). A new bathymetry grid has also been developed for the gravity data to process accurately the Bouguer and terrain corrections. This bathymetry grid has been built from the GEBCO 1' global bathymetry grid where datasets from a wide range of sources were incorporated.

3.1.2 Gravity Grids

GETECH assembled three types of gravity grids as its final deliverables to Petronas. Only two types of gravity grids were adopted from the GETCH global gravity data for the purpose of this study. They are: -

a) BAFA

The BAFA grid consists of Bouguer anomaly gravity data onshore and free air gravity data offshore.

b) BABA

The BABA grid consists of both onshore and offshore Bouguer anomaly data. The Bouguer anomaly values offshore were calculated using a rock density of 2.2 g/cc (density contrast of 1.17 g/cc) and terrain corrections were also applied.

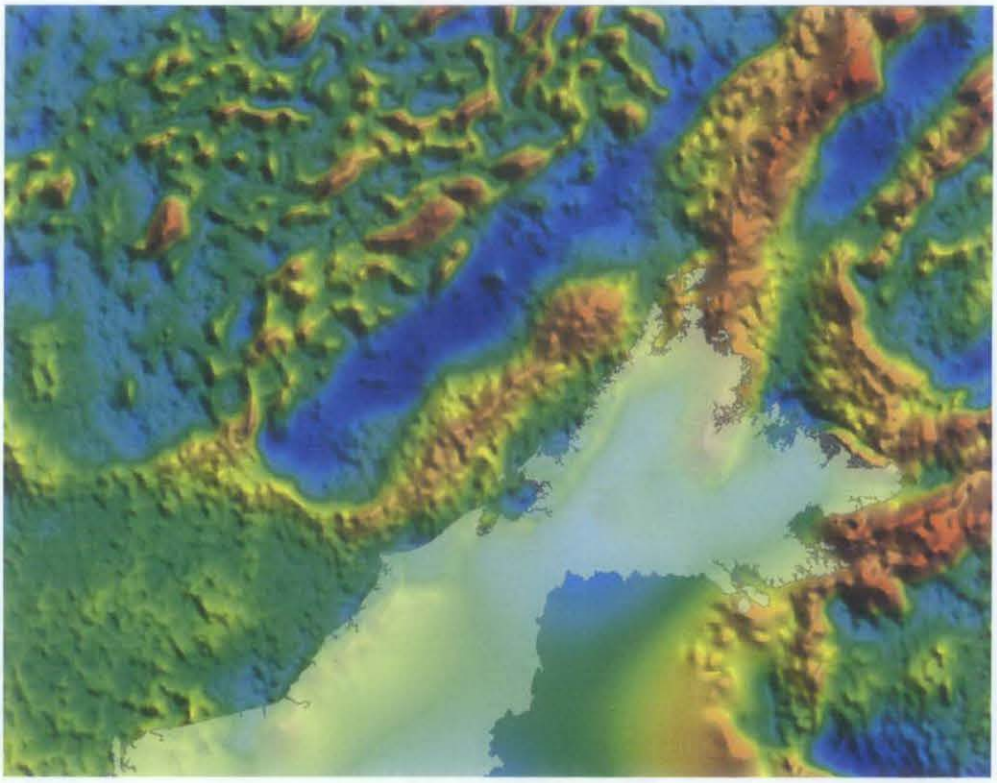

Figure 3.1: A raster image of the free air gravity data of the study area acquired from GETECH's Global Gravity Database.

The gravity grid of the study area was accessed using a grid extraction program designed by GETECH. The grid was extracted and output into ASCII format in xyz arrangement. The data extracted for the study area is located within lower left coordinates Latitude 2^{o} north and Longitude 110^{o} east, and upper right coordinates Latitude 10^{o} north and Longitude 120^{o} east. The data was processed in ArcGIS software and was interpolated into surfaces maps such as Triangular Irregular Network (TIN) and contour maps for visualization.

3.1.3 GETECH's Data Processing and Gravity Conversion

GETECH performed a processing sequence to the satellite gravity data in the Global Continental Margins Gravity Study which included waveform picking, data correcting, editing, and levelling to produce the best possible sea surface height grid. During this process, the data was also corrected for various environmental effects (e.g. troposphere, ionosphere, tidal etc).

Following this processing stage was converting data which was in sea surface height, to gravity. Here, the Brun's equation as listed below was used to relate gravity potential with the geoidal height:

$$N = T_P / \gamma_Q$$

where γQ is the normal gravity calculated at point Q on the ellipsoid using the ellipsoidal gravity formula, N the geoidal height, and T_P the gravity potential at point P (Figure 3.2). Point Q on the ellipsoid is where the normal to the ellipsoid passes through P.

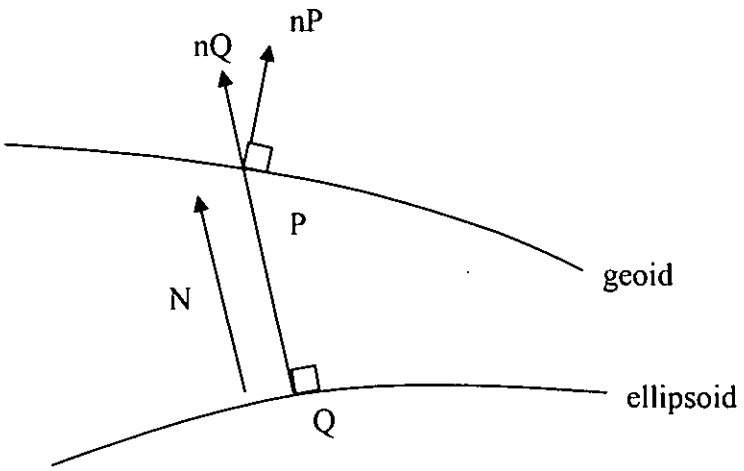

Figure 3.2: Relationship of point P on the geoid and point Q on the ellipsoid. N is the geoidal height and nP and nQ are the normal directions of the geoid and the ellipsoid respectively (After GETECH, 2007).

The normal gravity at point P is defined as the difference between the observed gravity at point P and the normal gravity at point Q.

$$\Delta gP = gP - \gamma_Q$$

As such, the gravity anomaly is essentially the vertical derivative of the potential which is proportional to the height of the geoid surface. The Fast Fourier transform (FFT) technique was used to convert geoidal data to gravity data.

3.2 Remote Sensing Data

3.2.1 Landsat Satellite Images

The satellite images used in the study are GeoCover 2000 datasets of Landsat Enhanced Thematic Mapper (ETM+) images with band 7-4-2. To cover the entire onshore section of the study area, as many as 7 scenes were acquired. They are as follows: -

a) N-50-05_LL_742_2000
b) N-50-05_LR_742_2000
c) N-50-00_UL_742_2000
d) N-50-00_LL_742_2000
e) N-49-00_UR_742_2000
f) N-49-00_LR_742_2000
g) N-49-00_LL_742_2000

Landsat Image Specifications (EarthSat, 2004) are as follows:-

i. Spectral bands: Three Landsat ETM+ bands with panchromatic band

a) Band 7 (mid-infrared light) is displayed as red
b) Band 4 (near-infrared light) is displayed as green
c) Band 2 (visible green light) is displayed as blue

ii. Coordinate System – Universal Transverse Mercator (UTM) / World Geodetic System 1984 (WGS84)

iii. Resolution : 14.25 meters

All the satellite images were downloaded from *https://zulu.ssc.nasa.gov*

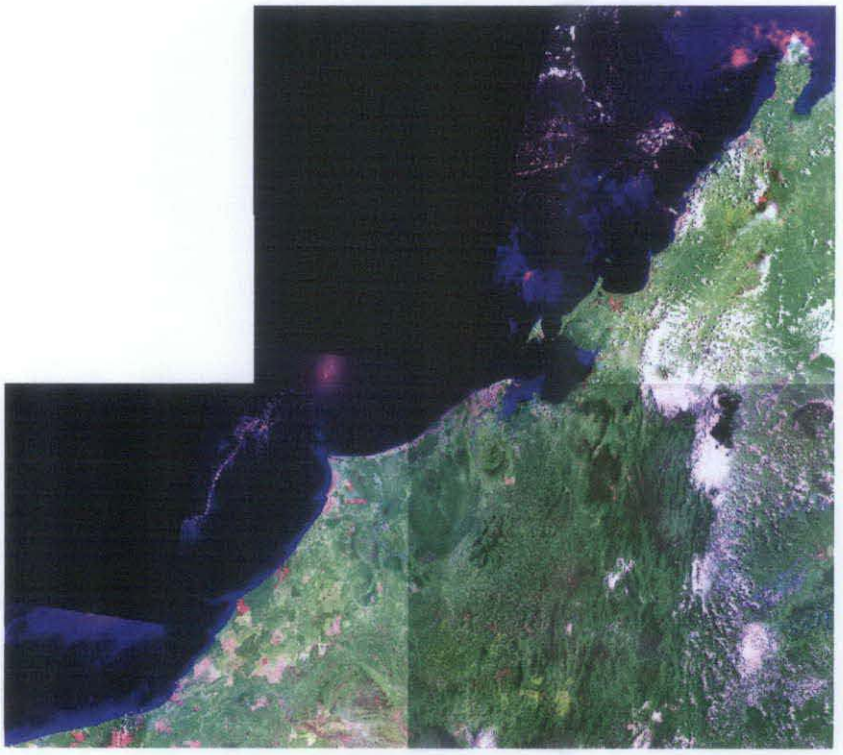

Figure 3.3: Landsat Enhanced Thematic Mapper (ETM +) image of the study area (NW Borneo) displayed in band 7-4-2.

3.2.2 Shuttle Radar Topographic Mission (SRTM)

For this study, SRTM data was used as the main source for topographic data. The SRTM data was downloaded from *http://srtm.csi.cgiar.org*. A total of 3 datasets were downloaded to cover the onshore section of the study area which is listed as below:

a) srtm_59_12
b) srtm_60_11
c) srtm_60_12

These data are SRTM 3 arc seconds coverage with 90 meters resolution. The SRTM data was downloaded in ASCII (X, Y, Z) format so that it could be imported into ArcGIS and processed into 3D Triangular Irregular Network (TINs), contour maps, hillshade maps and also into raster images.

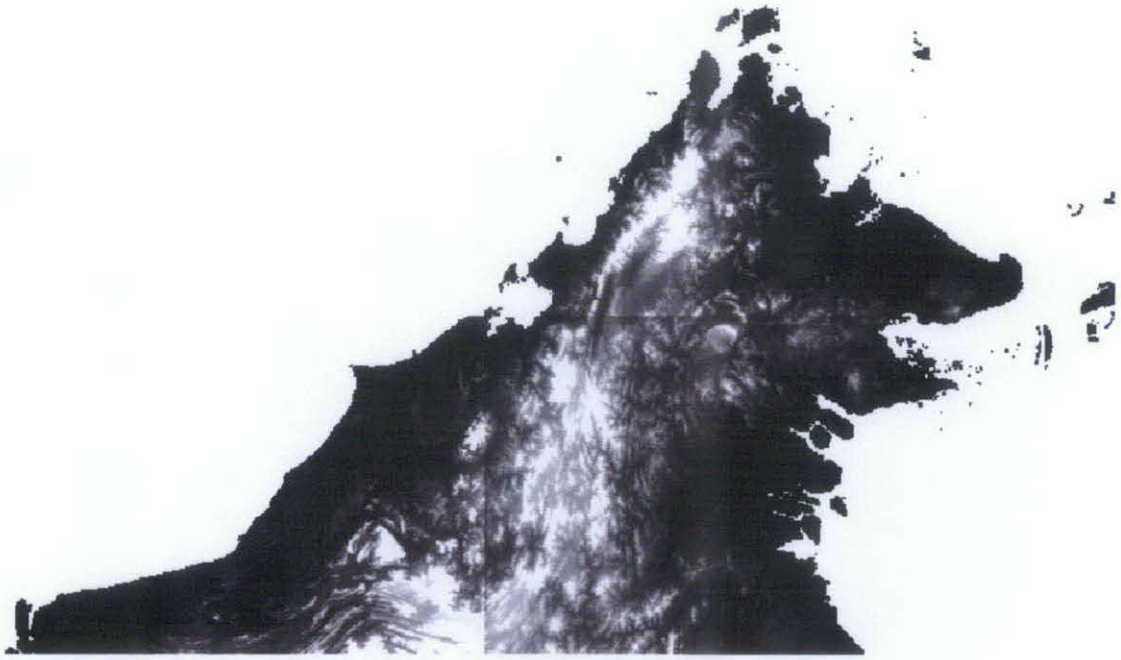

Figure 3.4: SRTM datasets covering the onshore section of the study area displayed in stretched black and white colour display

3.3 Bathymetry Data

A global bathymetry grid was also produced as a part of GETECH's Global Gravity Database that was compiled for Petronas. GETECH used this global bathymetry grid for the conversion of free air anomaly to the Bouguer corrections. This grid was produced from compilations from various sources such as GEBCO Digital Atlas (GDA), or alternative sources like digitized nautical charts, and also from GETECH's database. For the study area of NW Borneo, the bathymetry dataset resolution is ~500m (GETECH, 2007).

.

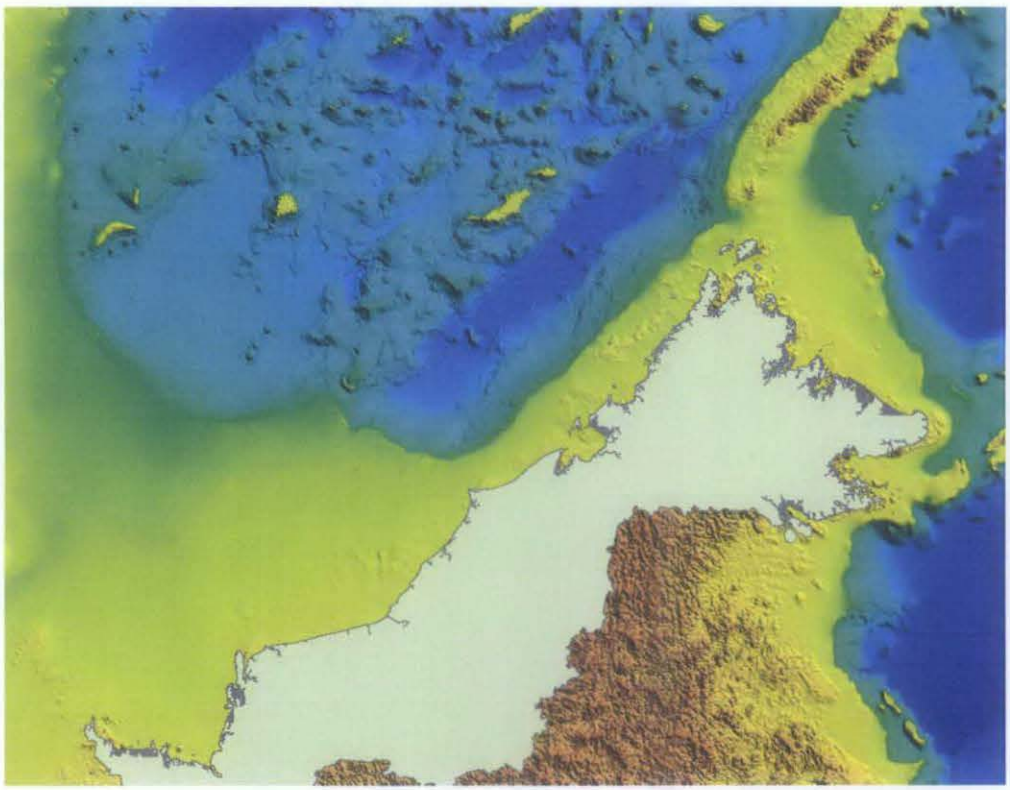

Figure 3.5: A raster image of the bathymetry data of the study area acquired from GETECH's bathymetry database.

Like the gravity grids, the bathymetry grid was extracted and output into ASCII format in xyz arrangement. The data extracted for the study area is located within lower left coordinates Latitude 2^{o} north and Longitude 110^{o} east, and upper right coordinates Latitude 10^{o} north and Longitude 120^{o} east.

The bathymetry data are acquired in ASCII (X, Y, Z) format. The data was processed in the ArcGIS software in order to be interpolated and viewed.

CHAPTER 4: METHODOLOGY

4.1 General Methodology

Like other GIS studies, the first stage is always data collection and preparation. During the data collection stage, an assessment was made to ensure that the data used was compatible with the GIS software. The assessment was not limited to investigating the spatial resolution, accuracy, reliability and availability of the data before it is selected for the study. Literature reviews on the various datasets used for the study have been made in Chapter 2. The data used for this study and its sources are explained in the previous chapter.

After the data had been selected and gathered, it had to be processed so that it could be visualized and used in the GIS software. As most of the data were acquired in ASCII format, several steps were required to interpolate the data into a format that the GIS software could display. The data preparation stage consisted of generating several surface maps for visual interpretation and data extraction.

A part of this study requires the interpretation of lineaments of the study area. Here, lineament interpretation was done visually on the Landsat images, and also on the other generated surface maps that was integrated and viewed concurrently. Here, the lineaments were interpreted as a layer or *shapefile* and stored in the GIS database.

The final part of the study involved gravity modelling, where a surface profile (topography/bathymetry) and gravity profile of the same line(s) were selected from the GIS and exported into a gravity modelling software, GM-Sys version 4.9. Using this software, the crustal properties (i.e. crust thickness\Moho depth, sediment cover etc.) was modelled and manipulated so that its gravity signature would match the observe gravity.

The findings made from both the lineament and gravity modelling analysis is discussed in the next chapter (Chapter 5).

4.2 Methodology

Below is the list of the steps used for this study: -

1) Data gathering and compilation
2) Creation of maps (TIN, contour maps, raster maps and hillshade maps)
3) Lineament Interpretation
4) Profile extraction for gravity modelling

4.2.1 Data gathering and compilation

The first part of the process involves data gathering on a GIS platform to integrate and view all of the data needed for the study. The datasets were also viewed to check its spatial extensions and geographic coordinate system; in this case the study was carried out using the WGS 84 coordinate system. The remote sensing images were also analyzed to determine the quality in terms of cloud cover, bands combinations, etc.

4.2.2 Creation of surface maps (TIN, contour maps and hillshade maps)

All of the datasets, with the exception of satellite images were acquired in ASCII (X, Y, Z) format. These data were needed to be processed and interpolated into *surface maps/models* before it could be visualized and used for analysis. Surface maps/models are able to facilitate the storage of surface information (Z values) into a GIS. A surface model also generates an approximation of the surface elevation by taking a sample of the values at different points on the surface and interpolating the values between these points.

For this study, surface maps will be generated to digitally represent the features of the different datasets used. The topographic data (SRTM) were generated into a surface of the study area that will be used for visualization during structural interpretation. A surface map of both bathymetry/topography and gravity was also generated for visualization and profile modelling where the Z component of the data will be

extracted from any cross section line. ArcGIS 3D Analysis extension was used to generate surface maps. Below is a list of surface maps generated from the datasets:-

a) Triangular Irregular Network (TIN)

The ArcGIS software stores this surface maps as a Triangular Irregular Network (TIN). TINs are a form of vector based digital geographic data and are constructed by triangulating a set of vertices (points). The vertices are connected with a series of edges to form a network of triangles (ESRI, 2006). The TIN is a digital representation of the surface generated because all Z information of all points will be stored in the TIN.

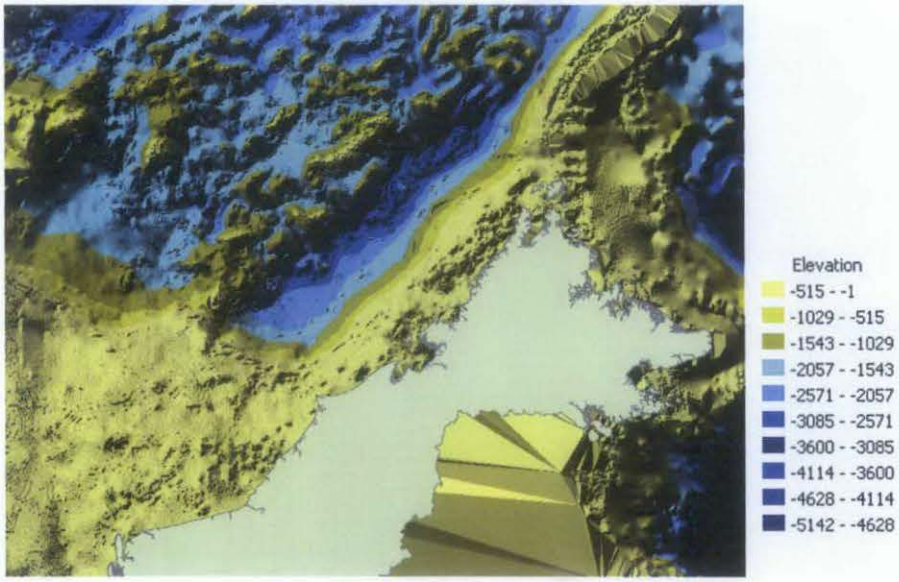

Figure 4.1: Generated TIN of bathymetry overlain by coastline polygon of NW Borneo. Colour scale (left) defined into 10 classes of elevation (scale in meters).

For this study, TIN maps were generated for bathymetry and gravity surface datasets. TIN maps were used to generate raster surface maps.

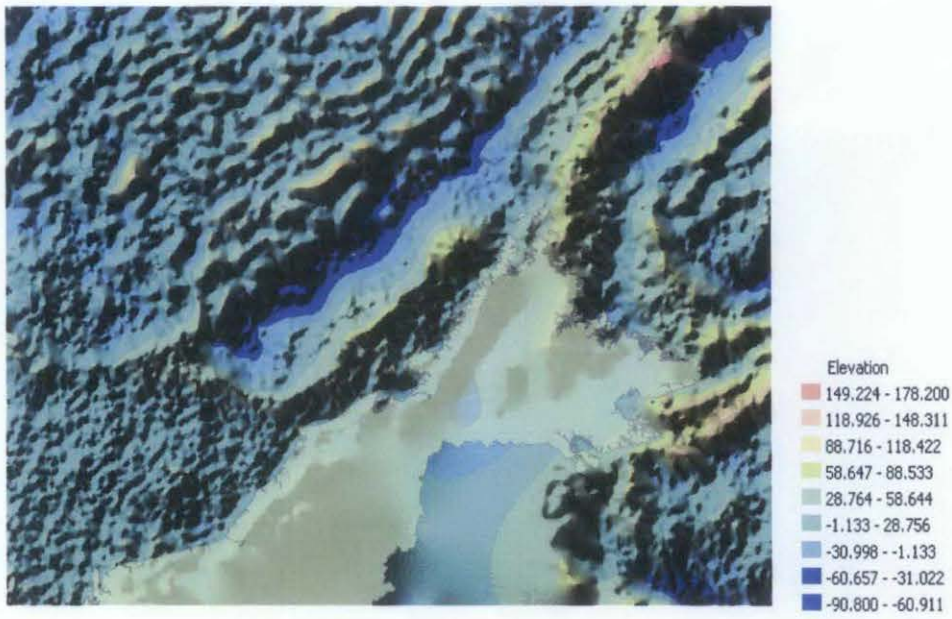

Figure 4.2: Generated TIN of free air gravity overlain by coastline polygon of NW Borneo with 30% illumination. Colour scale (left) defined into 10 classes of elevation (scale in mGal).

b) Contour Maps

Contour maps were made using the STRM data to assist visualization during the lineament interpretation. This map was generated with contour intervals of 100 m.

Figure 4.3: Contour map of the onshore region of NW Borneo. Contour in 100 m interval. Scale in meters.

c) Hillshade maps

Hillshade maps (Figure 4.4) are a shaded relief representation of a surface (ESRI, 2006). Hillshading allows visualization of a terrain of surface by simulating shades or shadows which is an effect of elevation or relief. Simulating shadows and shades can be done by applying an illumination at a defined angle and altitude. This illumination angle and altitude can be changed according to the user's specifications to enhance the terrain visualization according its characteristics.

Figure 4.4: Hillshade map created using illumination from altitude 45 degrees and azimuth of 315 degrees

c) Raster maps

Once the z values from the ASCII data sets are interpolated to the TIN, it was also able to convert the TIN to a raster file that also displays the elevation values using a colour scale bar. Raster files are faster to display as compared to TINs, and also can be displayed in 3D (Figure 4.6) using the ArcScene extension of ArcGIS. Both the bathymetry and gravity TINs are converted to raster (Figure 4.5, 4.6).

Figure 4.5: Raster interpolation of bathymetry map from TIN displayed with a hillshade map of Borneo.

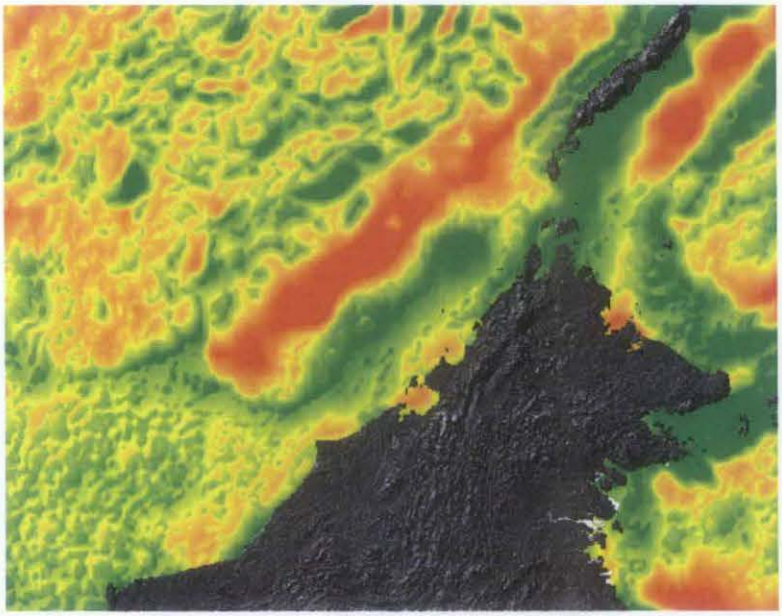

Figure 4.6: Raster interpolation of gravity map from TIN displayed with a hillshade map of Borneo.

4.2.3 Lineament Interpretation

As defined in the Chapter 2, lineaments are more or less rectilinear alignment features that can be seen on satellite images, aerial photographs and digital elevation models. For this study, only structural or tectonically related lineaments were interpreted. For this study, lineaments were interpreted visually on the Landsat image and SRTM derived surface maps (i.e. contour and hillshade). For better visualization, contour and hillshade maps were viewed concurrently with the Landsat images. This method provided better discrimination between tectonically induced lineaments and other non-tectonic induced lineaments (i.e. roads, artefacts, etc).

A more detailed explanation on lineament interpretation is discussed in Chapter 5.

4.2.4 Profile extraction for gravity modelling

A surface profile from the GIS was used as input into the gravity model; i) the bathymetry/topography surface, and ii) the gravity surface. Common cross-section lines were designed on both the surfaces and the profiles (Z values) of the lines and were exported to the gravity modelling software as separated profiles (gravity and topography/bathymetry) into the gravity modelling software. These processes are explained in detail below: -

a) Cross-section design

A cross-section line was designed on the GIS, mainly located specifically to cross the Sabah Basin, NW Sabah Trough and the Dangerous Grounds (Figures 4.7, 4.8). By overlaying the well density map and petroleum acreages, the line was also located to cross these oil prolific zones and also future exploration areas.

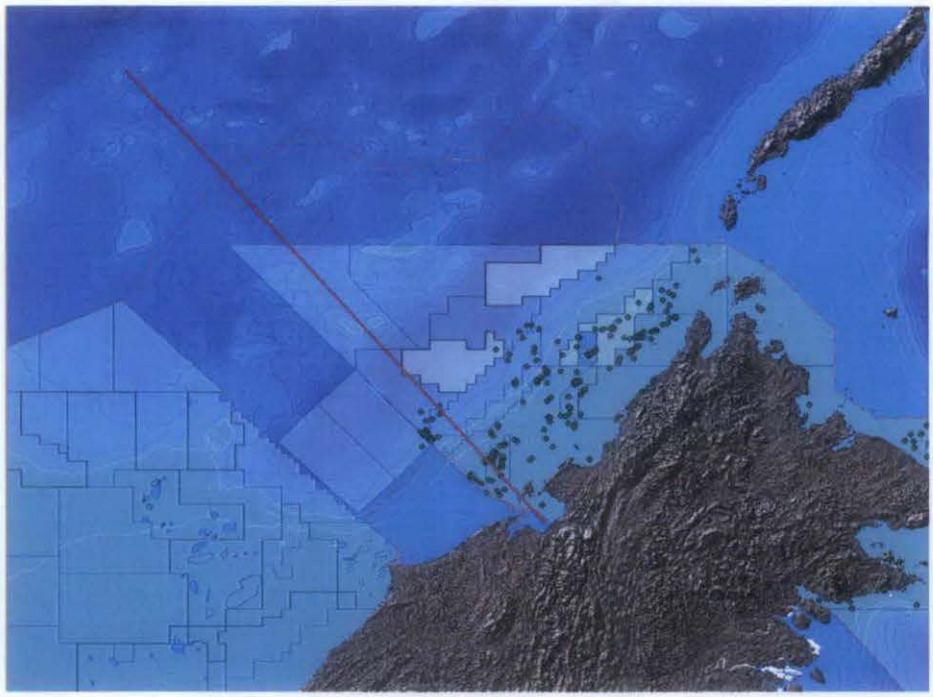

Figure 4.7: Cross-section lines (red line) designed with reference to the bathymetry map, and also well density and petroleum acreage blocks.

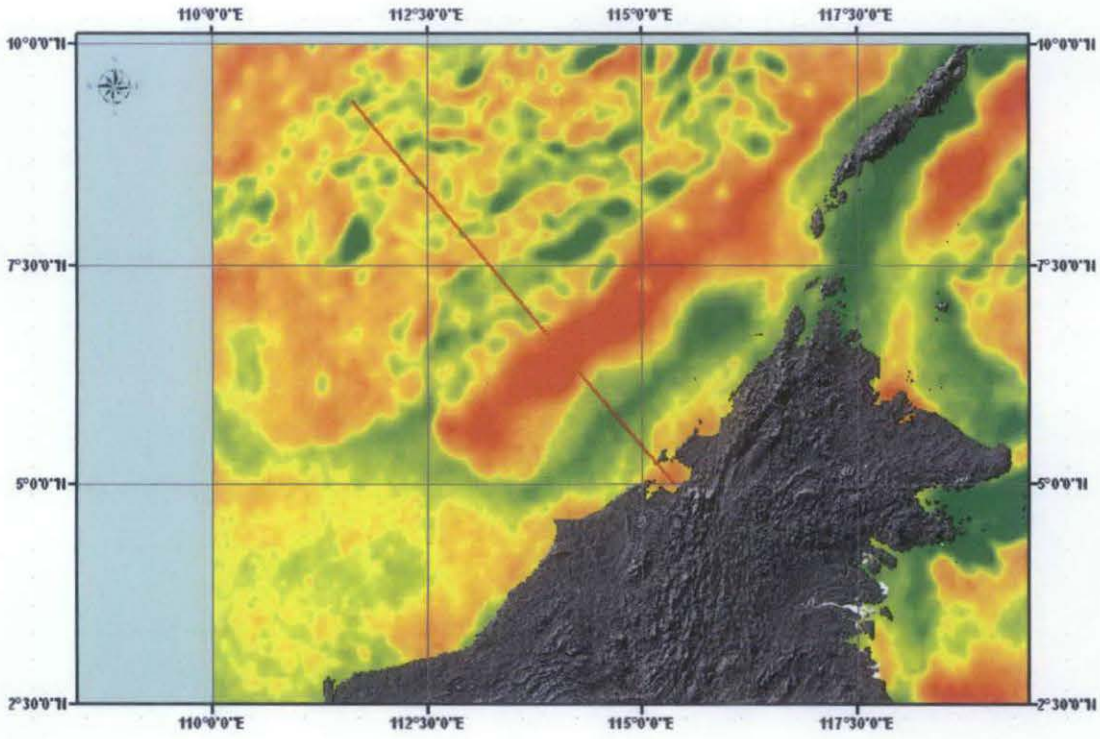

Figure 4.8: Cross-section lines (red line) designed with reference to the gravity anomaly map.

b) Assigning Z values to cross-section lines.

Once the line was created, it was merged with the earlier created TIN image of the gravity surface and the topography/bathymetry surface so that the z values of each surface at the line location could be stored in the database of the cross-section line. This was done using a function of ArcGIS 3D Analyst called "Convert Features to 3D" (Figure 4.9). For this operation, the input feature was the cross-section line, and the input 3D surface was the TIN models of the surfaces of gravity and bathymetry/topography. This process was done to assign the surface height to the cross-section line database (Figure 4.10).

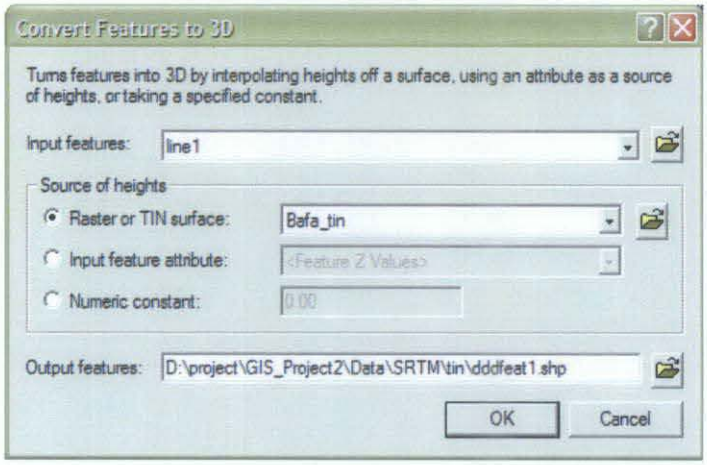

Figure 4.9: A menu display of the Convert Features to 3D function of ArcGIS 3D Analyst. The input features box is set as the cross-line (Line 1) and the source of height (Z values) is set as one of the TIN surface models (Bafa_tin)

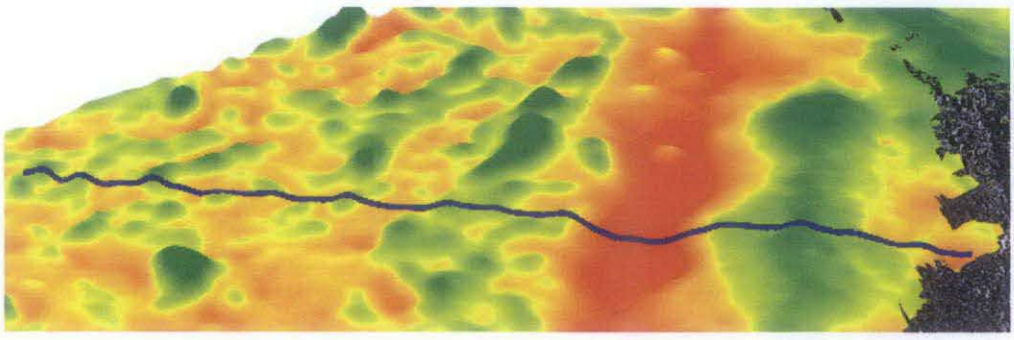

Figure 4.10: The cross-section line (viewed in 3D) draping over the gravity surface after assigning height values to the line.

c) Converting cross-section lines to points

In ArcGIS, line shapefiles are defined by its start and end point coordinates. As profiles are needed to be defined as a series of points with its X and Y coordinates and Z values, it is necessary to convert the line into point shapefile so that all Z values can be assigned to its X and Y coordinates. For this process, the line was spliced into vertices by a defined sampling interval, and after that the vertices were then converted to points. These were carried out using ET Geowizard version 9.6.1 which is an extension software created for ArcGIS. The sampling interval used for the conversion was 0.009 decimal degrees. This was equivalent to ~1000m if it was projected to the Universal Transverse Mercator (UTM) projection (Figure 4.11).

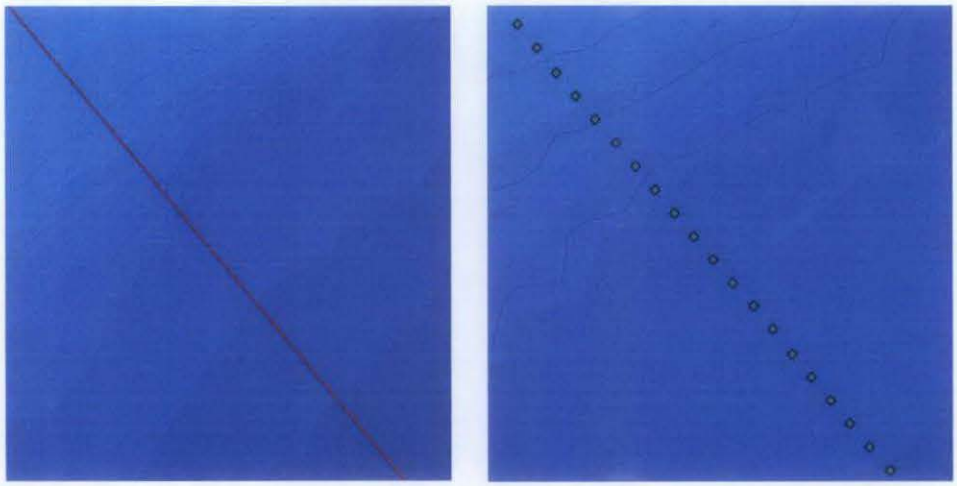

Figure 4.11: The cross-section line converted to a point shapefile, with 0.009 decimal degrees which is equivalent to ~1000 m interval.

d) Exporting profiles to Gravity modelling software (GM-Sys)

After the line had been merged with the surfaces and converted to points, all of its attributes would be stored in a database (**.dbf*) file. The Z-values of a cross-section line (i.e. Line1) can be retrieved in its database file (i.e. Line1.dbf).

Using *Microsoft Excel* software to view and manipulate the file, the coordinates were converted into distances using the northwesternmost point which was the first point (distance = 0 m). With the distance calculated, the file was then exported into an

ASCII file with the arrangement of *point ID, distance (m), topography height (m) and gravity (mGal)*. The ASCII file is then imported into GM-Sys software for gravity modelling.

Table 4.1: Attributes (Point ID, and its X, Y, Z coordinates) listed in a cross-section database file (i.e. Line1.dbf). The Z values are the result of merging line with a TIN surface.

	A	B	C	D
1	ET_ID	ET_Z	ET_X	ET_Y
2	0	-34.01701	657230.12098	561108.06804
3	1	-35.14559	656576.66652	561860.15802
4	2	-35.92723	655923.22521	562612.25029
5	3	-36.70887	655269.79707	563364.34490
6	4	-37.12869	654616.38211	564116.44185
7	5	-37.27566	653962.98036	564868.54118
8	6	-37.10705	653309.59184	565620.64290
9	7	-36.74672	652656.21656	566372.74705
10	8	-36.06525	652002.85455	567124.85364
11	9	-35.38378	651349.50583	567876.96271
12	10	-34.24527	650696.17042	568629.07426
13	11	-32.39463	650042.84834	569381.18834
14	12	-30.54399	649389.53961	570133.30495
15	13	-28.94991	648736.24425	570885.42413
16	14	-27.61037	648082.96228	571637.54590
17	15	-26.27083	647429.69373	572389.67029
18	16	-24.54479	646776.43860	573141.79731
19	17	-23.21494	646123.19693	573893.92699
20	18	-22.12254	645469.96873	574646.05936
21	19	-20.92242	644816.75403	575398.19443
22	20	-19.65965	644163.55283	576150.33224
23	21	-18.42098	643510.36518	576902.47281
24	22	-16.45762	642857.19107	577654.61616
25	23	-13.97888	642204.03055	578406.76231
26	24	-11.38605	641550.88362	579158.91129
27	25	-10.92558	640897.75030	579911.06313
28	26	-10.80859	640244.63062	580663.21784
29	27	-10.70058	639591.52460	581415.37545
30	28	-9.54260	638938.43226	582167.53599
31	29	-7.15997	638285.35362	582919.69947
32	30	-2.74724	637632.28869	583671.86593
33	31	-3.06468	636979.23750	584424.03539

Table 4.2: Final ASCII file aligned as point ID, distance (m), topography height (m), gravity (mgal).

line1_final.txt - WordPad

File Edit View Insert Format Help

0	0	-40	32.276
1	996	-40	30.75
2	1991	-40	29.672
3	2987	-39	28.633
4	3983	-39	28.235
5	4979	-42	28.198
6	5974	-44	28.174
7	6970	-43	28.481
8	7966	-43	29.101
9	8961	-43	29.519
10	9957	-43	29.914
11	10953	-43	30.785
12	11948	-43	31.608
13	12944	-42	32.39
14	13940	-41	33.995
15	14935	-38	35.605
16	15931	-32	37.346
17	16926	-22	39.374
18	17922	-14	41.335

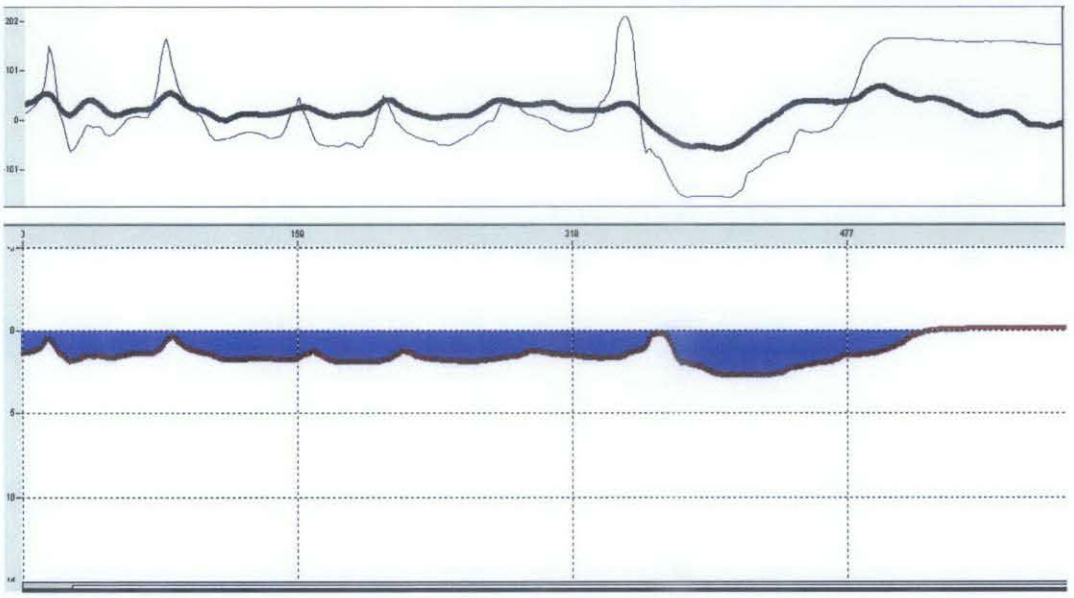

Figure 4.12: Results of the exported profiles of gravity (above) and bathymetry (below) displayed in GM-SYS V 4.1 software.

CHAPTER 5: ANALYSIS AND RESULTS

5.1 Lineament Analysis

Chapter 4 explains how the SRTM data and Landsat image were manipulated to produce better visualization for lineament interpretation. Using the GIS tools, the SRTM data were processed to produce hillshade maps and contour maps, whereas the Landsat images were displayed transparently and concurrently with the contour map to produce a better display for lineament interpretation.

5.1.1 Lineament Interpretation

The linear features identified in the study area included topographically negative lineaments, represented probably by faults, synclines, shear zones, drainage, and topographically positive lineaments that could be associated with folds (axis). Even though linear features could also be identified in the Landsat images, it was found that in the study area, using only the Landsat image was not sufficient to distinguish between positive and negative topographic lineaments.

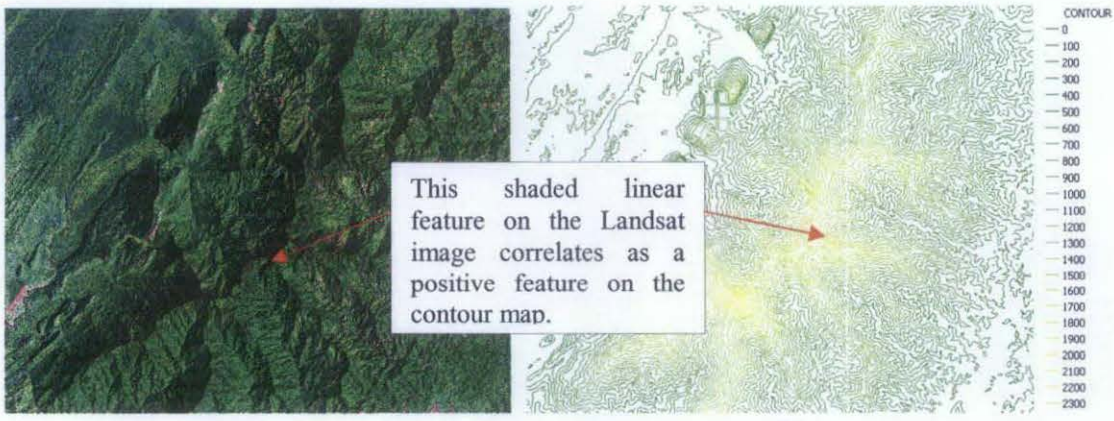

(a) **(b)**

Figure 5.1: (a) Cropped image from the Landsat data and (b) contour map of the same area. The dark shaded linear feature crossing through (a) would have been interpreted as a negative feature whereas it is shown as a positive feature on (b). Contour in meters.

The presence of thick vegetation or water bodies could also affect the image visualization. In certain areas, negative features (e.g. ravines) could instead be misinterpreted as positive features (e.g. fold axis) instead (Figure 5.1).

Figure 5.2 shows the folds interpreted using the Landsat images and guided by contour maps. Figure 5.3 shows the visualization of Landsat images with contour maps viewed concurrently. Linear features that appeared with higher contour values could be distinguished as folds. Fold axes can be distinguished from adjacent synclinal axes or any other features along strike. Eroded and exposed bedding along the strike of the folds would also appear as candidates for lineaments.

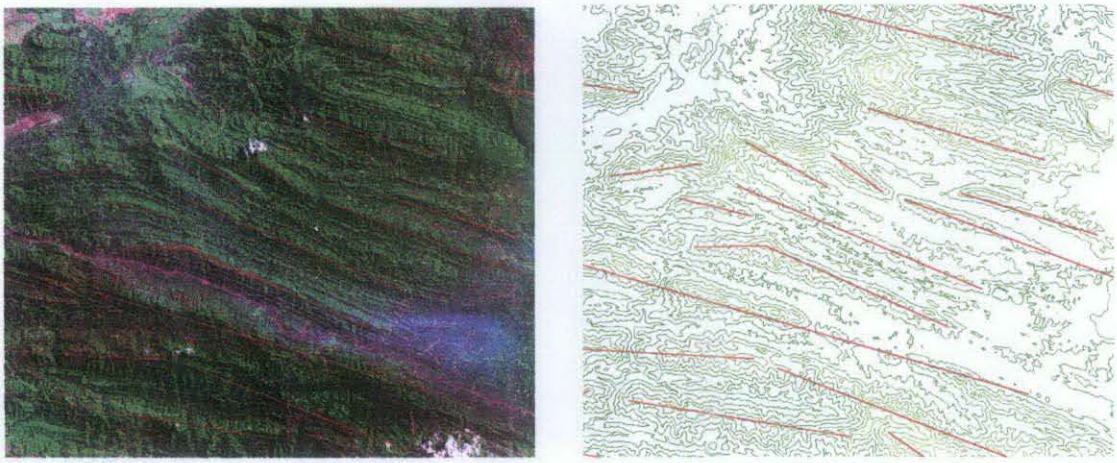

(a) **(b)**

Figure 5.2: Lineament interpretation (red lines) represented by folds of an area in the Landsat image (a) guided by the contour map (b).

Hillshade maps provided good visualization for identifying fold structures. An illumination azimuth was set as right-angles to the fold orientation to simulate shadows associated with the fold relief (Figure 5.4). For this interpretation, illumination azimuths of 315° N, 0° N and 45° N were used to create hillshade maps (Figure 5.5).

The other linear features interpreted were also represented by shear zones, faults and fractures. These features were both interpreted on the Landsat images (Figure 5.6a) and hillshade maps (Figure 5.6b). The detection of these lineaments also benefited

from the usage of varying illumination angles of the hillshade maps. Lineaments would also appear darker due to the generated shades from the structure.

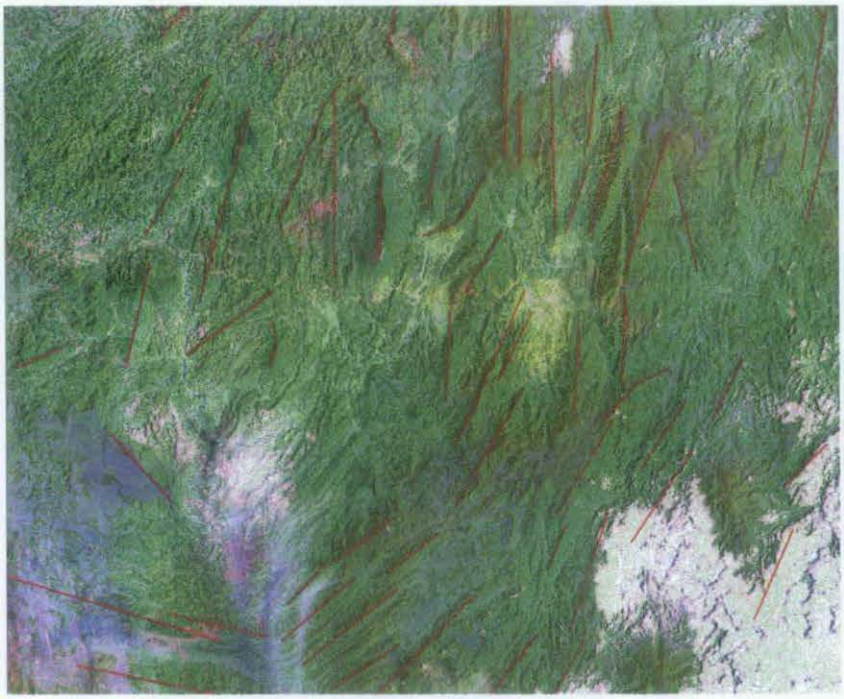

Figure 5.3: The Landsat image applied with 30% transparency and overlain above the contour map. Lineaments are marked as red lines.

Figure 5.4: Lineaments (red lines) interpreted as folds in the hillshade map.

Faults would create a shaded area adjacent to the relief and opposite to the illumination azimuth. Lineaments were also seen as cross-cutting linear features which could be represented by shear zones (Figure 5.7). Interpreting lineaments on Landsat images have disadvantages when an area is covered by vegetation or clouds, as it makes linear features harder to be detected. In this areas, the SRTM derived hillshade maps were used to compliment the Landsat images as SRTM data are not affected by clouds and vegetation (Figure 5.8).

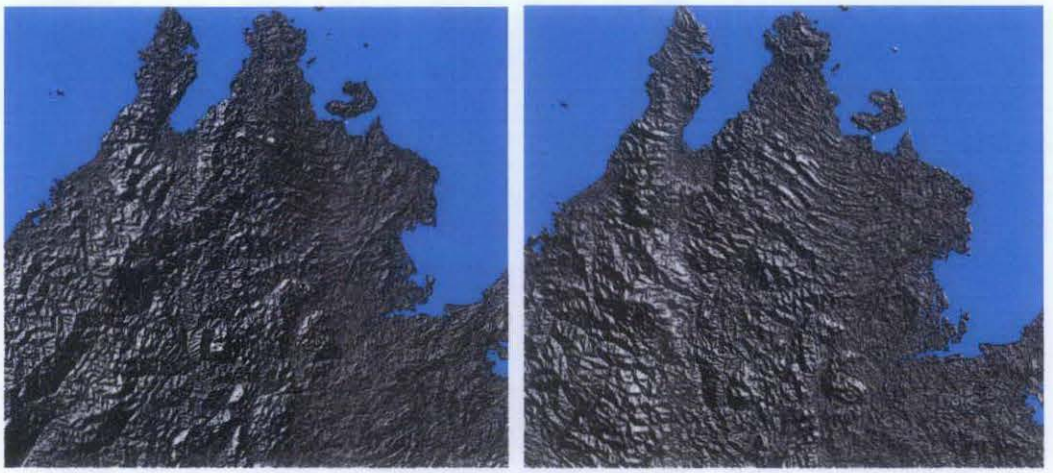

(a) (b)

Figure 5.5: Hillshade map of Sabah created using illumination azimuths of 315° N (a), and 45° N (b). Different illumination angles can be used to detect lineaments in different orientation.

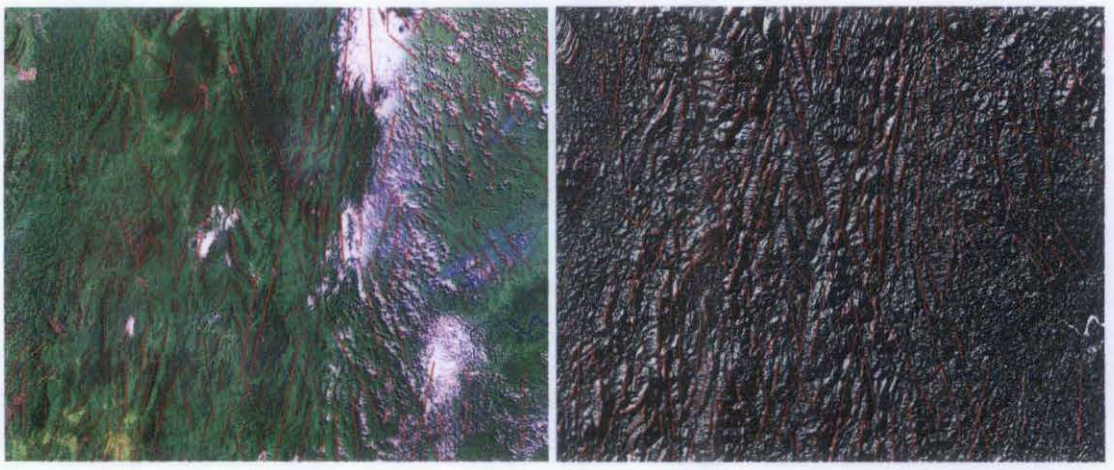

(a) (b)

Figure 5.6: Lineaments (red lines) interpreted on a portion from a Landsat image (a) and on the corresponding hillshade map (b). Lineaments not visible on (a) due to cloud cover are resolved on the hillshade map (b).

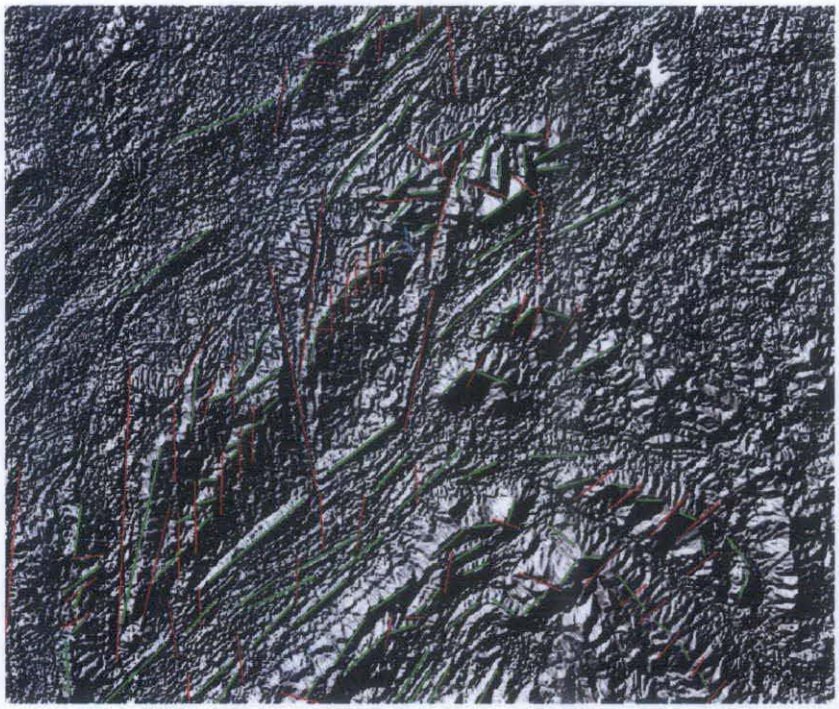

Figure 5.7: Lineaments represented by shear zones (red lines) seen as cross-cutting other linear features (green lines) interpreted on the hillshade maps.

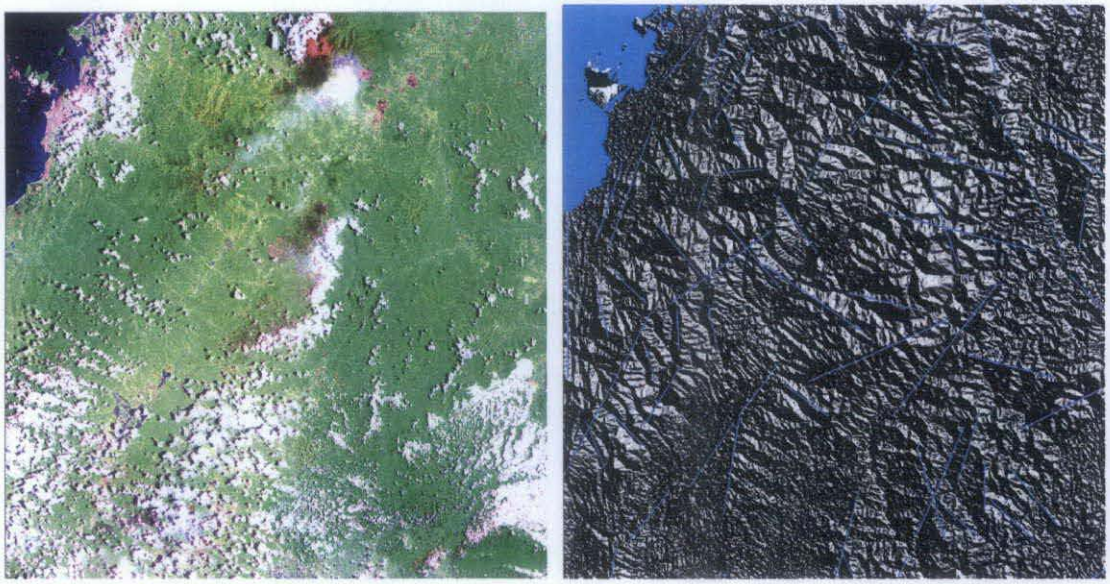

(a) **(b)**

Figure 5.8: (a) Landsat image of an area covered by thick vegetation and cloud cover where detection of lineaments was difficult. (b) Hillshade map of the same area but unaffected by clouds and vegetation. Blue lines are interpreted lineaments.

Figure 5.9: Final lineament interpretation (blue lines) displayed on the hillshade map of the study area.

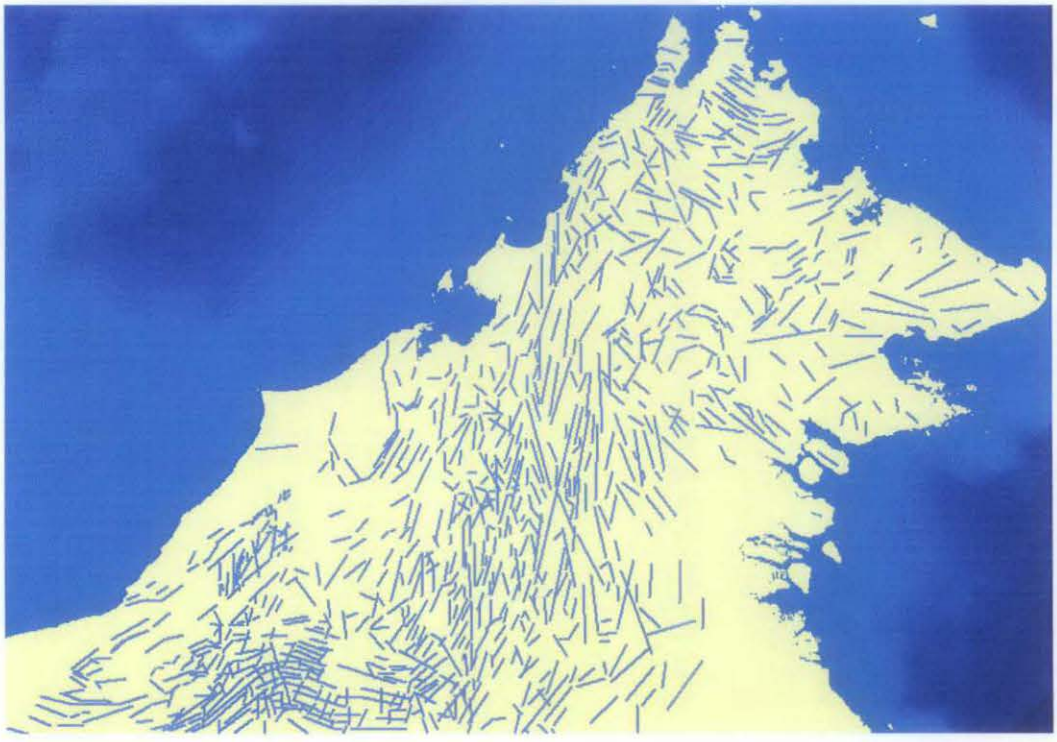

Figure 5.10: Final lineament interpretation (blue lines) displayed on the coastline map of the study area.

5.1.2 Analysis of the lineament trends

There is a general trend of lineaments (Figure 5.9 and 5.10) evolving from the southwestern region to the north of the study area. These lineaments represent the interpreted fold structures of the Rajang-Crocker Fold-Thrust Belt, which is greatly expressed in the study area. This trend extends from southwest of Sarawak to north of Sabah and forms a large S-shape pattern (Benard et al., 1989). It begins in the south west of the study area in an E-W (~ N80 degree) trend and gently diverting to ~ N50°-N55° north-eastern direction, nearly similar (parallel) to the change of coastline direction of Sarawak. In the central part of the study area, the whole trend changes abruptly northwards to a ~N10°-N20° trend.

In this region, the majority of the lineaments are long and oriented north easterly as mentioned. However, a few lineaments were observed to be in a north westerly (~N350 degree) direction and seem to be cross cutting the north-easterly trending lineaments. In this region, the lineaments however are not parallel to the shoreline. In the Sabah region (Crocker Range), ~5°N Latitude, the general lineament trend starts to gently move eastward, almost parallel to the Sabah western coastline. At the tip of the region, the lineaments seem to change south easterly and are parallel to the north east coastline of Sabah (Palawan Sea).

The dynamic change in orientation of the fold trend could be an evidence of multiphase tectonic evolution (Bernard et al., 1989; Tongkul, 1999). As describe in Chapter 2, the fold and thrust belt were formed by subduction processes since Late Cretaceous which also led to the different episodes of tectonic collisions involving the Luconia Block and Dangerous Grounds.

E-W orientated lineaments southwest of Sarawak could mark the folds formed by the southward subduction of the Rajang Sea. The NE-SW oriented lineaments in the central region of the study area could be related to the northwestwards facing thrust-folds resulting from the collision of the Luconia Block with Borneo. In Sabah, N-E orientated lineaments mark the uplifted Crocker formations.

Another evidence of multiphase tectonic evolution is the occurrence of lineaments that cross cut the fold trends. These lineaments vary in orientation from NW-SE to N-S trending (Figure 5.11), which could be wrench faults or shear zones that result from changes in tectonic compression orientation, probably related to the opening of the South China Sea Basin.

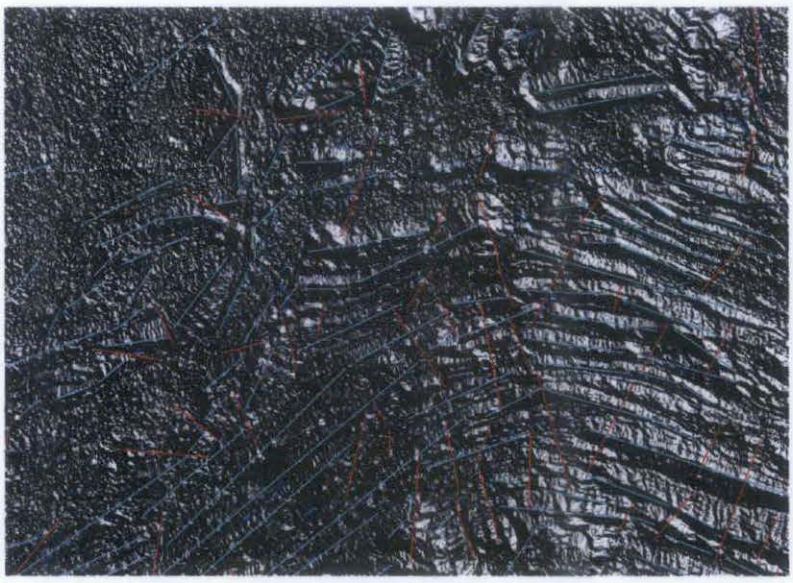

Figure 5.11: Strike-slip faults interpreted as red lineaments seen as cross-cutting the fold trend in blue lineaments seen on the southwest part of the study area.

5.2 Gravity Modelling

The GIS was applied as a platform for gathering several datasets (i.e. gravity, bathymetry), and furthermore, specific information from areas of interest could be extracted for further analysis. In Chapter 4, a line was designed to cross several areas in the offshore region of the study area and merged with its intersecting bathymetry and gravity coverage to produce cross-section profiles of both bathymetry and gravity. This section will discuss about the gravity interpretation and modelling made using the extracted data from the GIS.

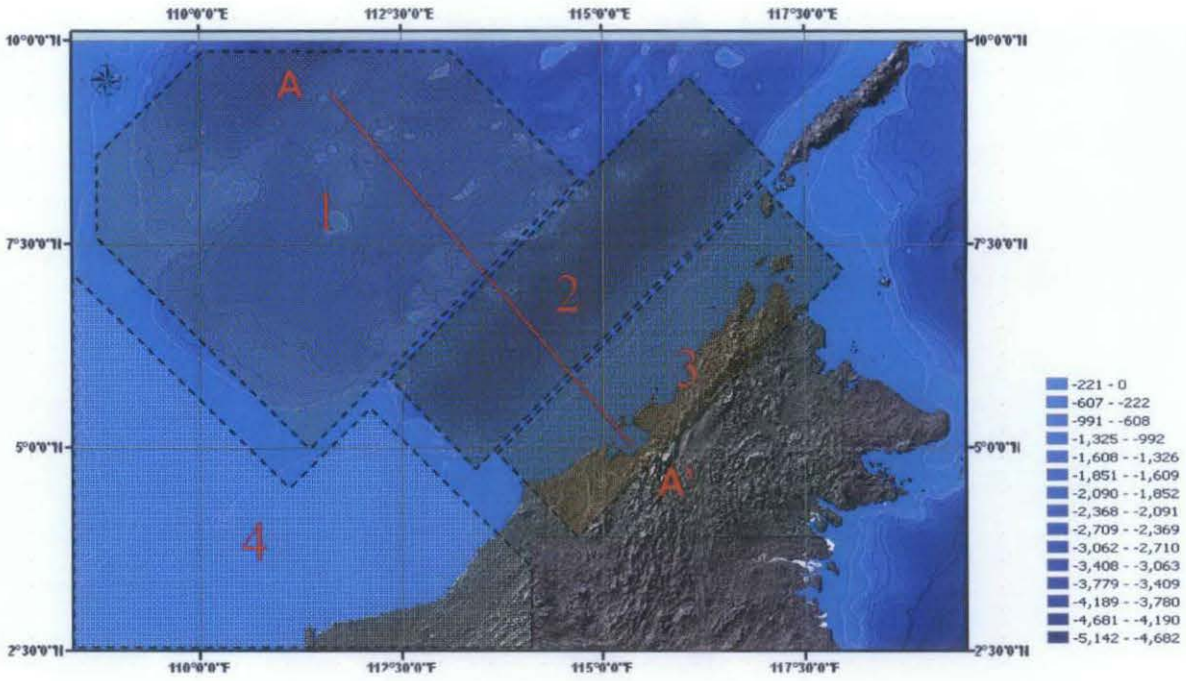

Figure 5.12: Line location displayed on the bathymetry map. Scale in meters. The labels refer to the respective physiographic features of the study area: 1 = Dangerous Grounds, 2 = Sabah Trough, 3 = Sabah Basin, and 4 = Sarawak Shelf.

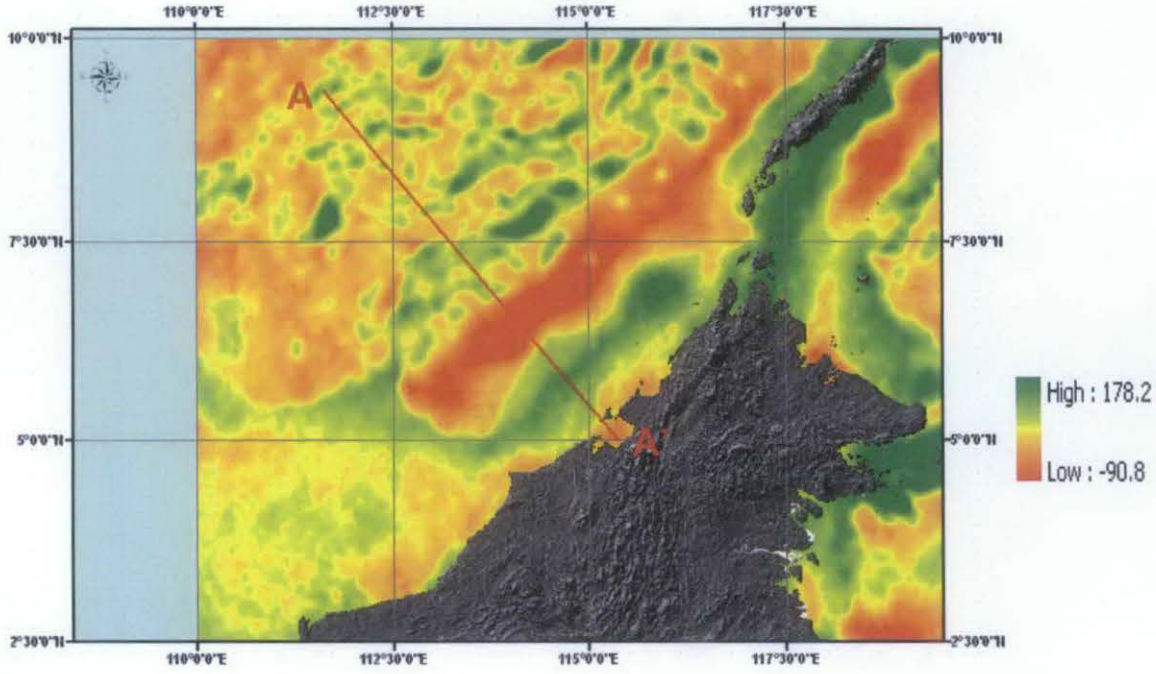

Figure 5.13: Line location displayed on the free air gravity anomaly map. Scale in mGal.

5.2.1 Line A

Line A (Figures 5.12 and 5.13) extends from point A, the NW Sabah Platform (Dangerous Grounds) and crosses through the NW Borneo Trough and the Sabah Slope and ends at the coast of Sabah (A'). The total length of the line is ~635 km. Figure 5.14 shows the profiles of the bathymetry and the observed free air gravity along line A.

The gravity anomaly ranges from ~ 60mGal to ~200mGal and the bathymetrical varies from 0 m to ~3km (Figure 5.14). The observed gravity curve is similar to the bathymetric curve which displays a high around the Sabah slope followed by a low in the Sabah Trough and a second high in the realm of the Sabah Platform (Dangerous Grounds) and beyond.

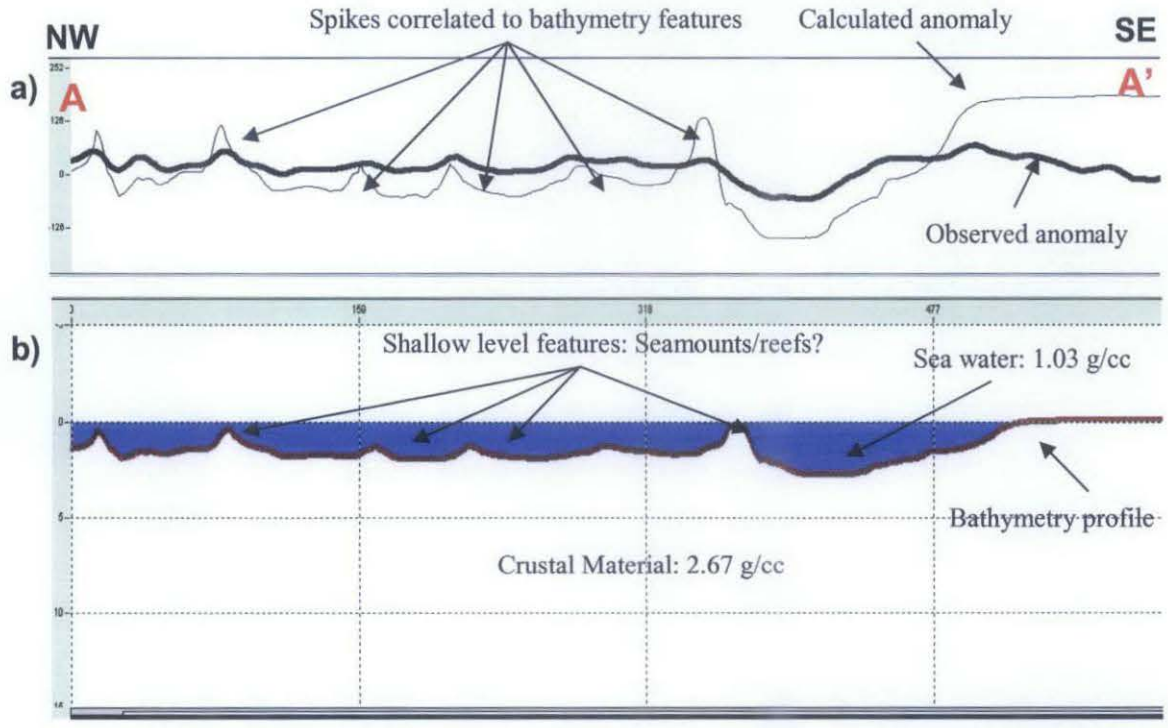

Figure 5.14: Profiles of the observed gravity (a) and bathymetry (b) across line A observed in the gravity modelling software. Observed gravity (thick line) and calculated gravity (thin line) for a density of 1.03 g/cc for seawater and 2.67 g/cc for crustal material below the bathymetry. Density contrasts between crustal material and seawater produce high amplitude and short wavelength calculated anomalies.

If a density value of 1.03 g/cc was applied to the seawater, and 2.67 g/cc was applied to the material below the bathymetric profile i.e. the crustal material, the calculated free-air gravity anomaly profile (Figure 5.14) would generally resemble, or be controlled by the sea floor bathymetry. High amplitude and short wavelength anomalies (spikes in figure 5.14) are most likely to be affected by high density contrasts at shallow levels, probably caused by volcanic seamounts and reefs.

As a comparison, the observed gravity profile however is generally smoother and has less exaggeration in amplitude. This could be an indication that the observed gravity anomaly is more likely to be caused by variations in density that occur deeper within the crust rather than simply due to the variations of the sea floor topography.

To investigate the effects of variations within the earth's crust on the gravity anomaly, the densities of the crust and mantle material, as well as the depth to the Mohorovicic discontinuity must be estimated.

5.2.2 Airy Isostatic Model

The Airy isostasy model was applied to compute the crustal thickness along the profile and hence the depth to the Moho. This model computed with the bathymetry input to determine the isostatic compensation along the profile. Other assumptions included no sedimentation cover, the density of water to be 1.03 g/cc, density of the crust 2.8 g/cc, and the density of the mantle 3.3 g/cc.

Besides the coastal areas of Sabah, (Crocker formation, south east of line) was assumed to rest in isostatic equilibrium with a crustal thickness (depth to Moho) of 35 km (Figure 5.16). Isostatic compensation was also made locally for this model. Figure 5.15 illustrates the Airy Heiskanen model of isostatic compensation.

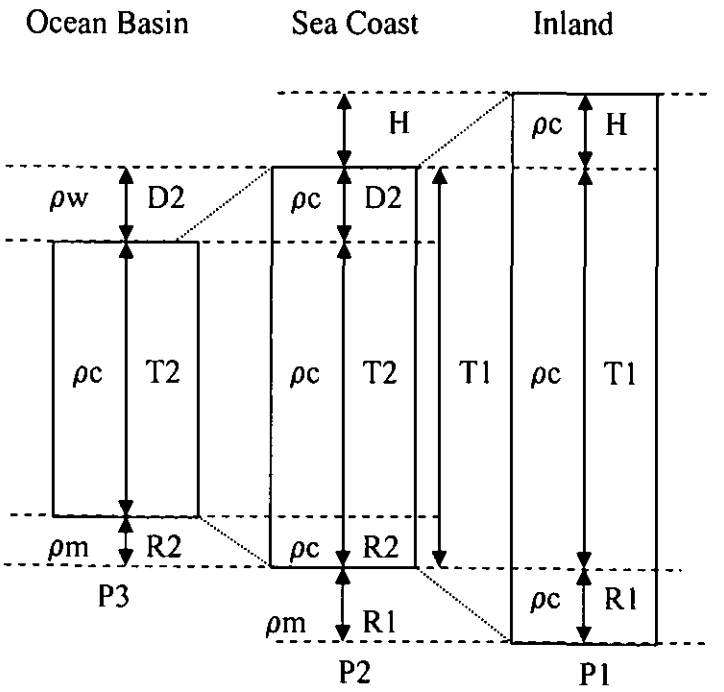

Figure 5.15: The Airy Heiskanen model for isostatic compensation. Modified from Watts (2001).

$P1 = (H + T1 + R1)\,\rho_c g$ and; $P2 = T1\,\rho_c g + R1\,\rho_m g$

Assuming isostatic equilibrium: -

$$\therefore \quad P1 = P2$$

$$\therefore \quad (H + T1 + R1)\,\rho_c g = T1\,\rho_c g + R1\,\rho_m g$$

$$\therefore \quad r = \frac{H\rho_c}{(\rho_m \cdot \rho_c)}$$

Work example: (i.e D = 500m, D + T + R = 35 000m)

$P2 = (35\,000\ m)\,\rho_c g$

$P3 = (500m.\rho_w g) + (T.\rho_c g) + (R.\rho_c g)$

$$\therefore \quad P2 = P3$$

$$\therefore \quad r = \frac{D.\rho_w - D.\rho_c}{(\rho_m - \rho_c)}$$

: r = 1770m

: so thickness of crust in basin = 35 000 – 500 – 1770

= 32 800 m

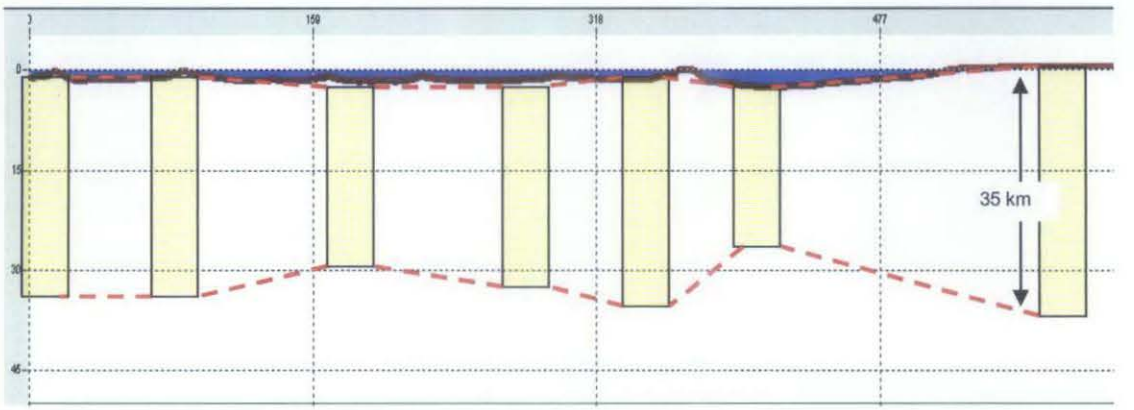

Figure 5.16: Assuming the crustal thickness onshore Sabah is 35 km, the principle of isostasy was used to estimate the thickness of the crustal columns across the offshore regions of the modelled profile.

The computed gravity anomaly trend generally agreed (Figure 5.17) with the observed gravity anomaly. Although the observed and calculated gravity values do not match, it was observed that the shapes of the two curves have a more or less similar tracking pattern. As expected, in relatively higher topographic areas (e.g. Sabah coast), the relatively greater thickness of the crust is compensated by relatively deeper Moho.

The deep basin of NW Borneo Trough is compensated by a higher Moho (thinner crust) and hence shallower level of a density contrast. It can be concluded that the theory of isostasy is applicable to this model to generate a general model of the crustal thickness (depth to Moho). However when investigating the differences (calculated vs. observed) in detail, some observations were made.

The Moho surface was also too undulated and unusual (Figure 5.17). Therefore, the surface was edited graphically using the editing options of the software to smoothen the surface. The intention of this step was similar to applying regional isostatic compensation, but not by detailed calculations methods (Figure 5.18).

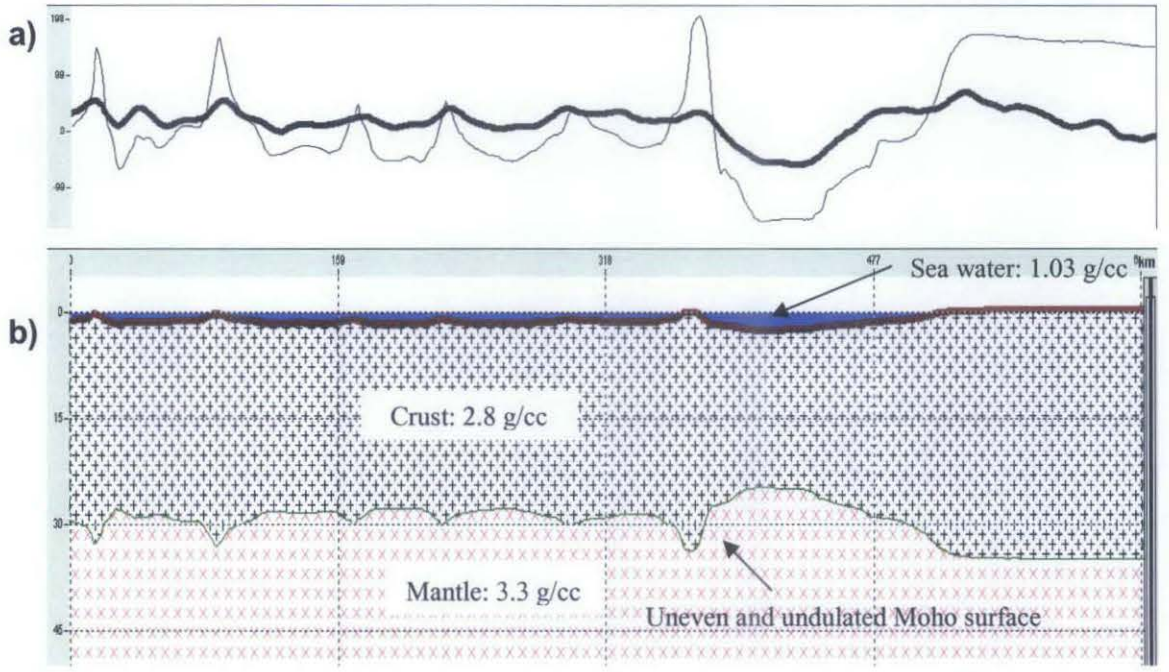

Figure 5.17: (a) Gravity profile resulting from applying isostatic compensation. (b) Depth to Moho (crust thickness) determined from isostatic computations.

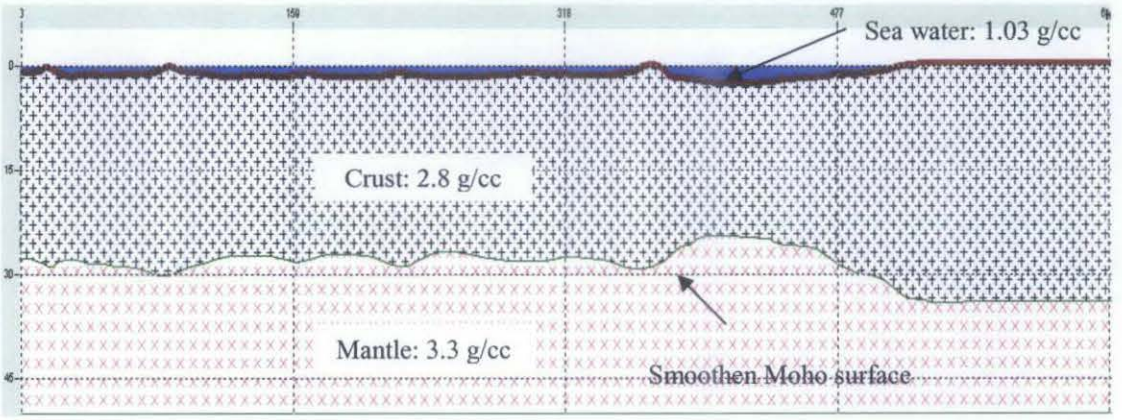

Figure 5.18: The resulting Moho surface after smoothing.

5.2.3 Crustal Thinning

In order to match the calculated gravity profiles at the underestimated areas in the Dangerous Grounds region, crustal thinning was attempted. To get a match, a crustal thinning factor of ~ 0.6 was applied for this region.

This would be similar to elevating the Moho by ~ 10 km. The final crustal thickness of the region after thinning would be ranging from ~15 - ~23 km (Figure 5.19). The crust underneath the Sabah Trough was also needed to be thinned by ~ 4 km (Figure 5.20).

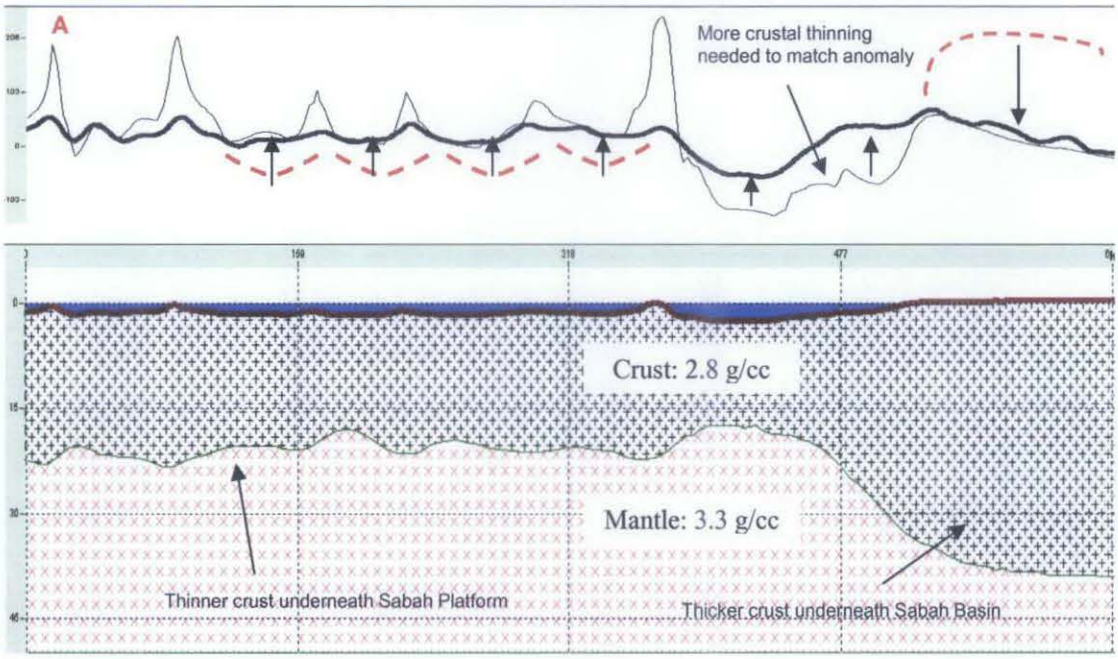

Figure 5.19: Crustal thinning applied below the Dangerous Grounds region. Gravity anomaly profile matching the observed gravity after crustal thinning was applied.

An elevated Moho would match several parts of the gravity lows in the Dangerous Grounds and Sabah Trough regions. However, the gravity highs (spikes) could not be attenuated to be matched by crustal thinning. Crustal thinning also resulted in the matching of the calculated gravity curve on the coastal region of Sabah.

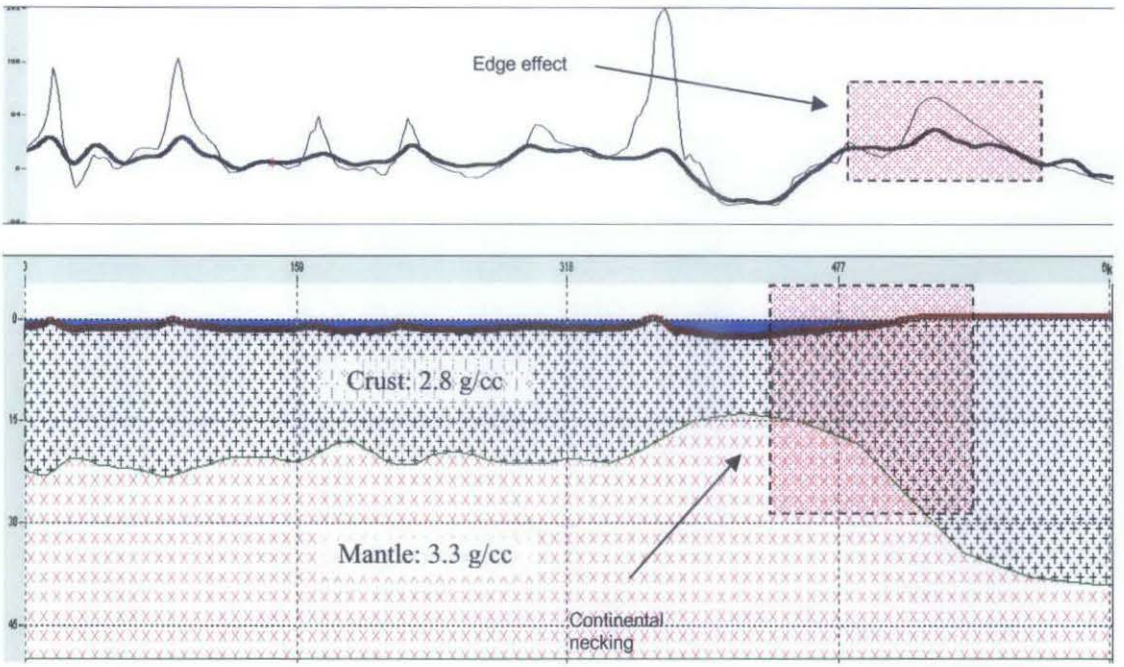

Figure 5.20: Crustal thinning applied below the Sabah Trough region. Gravity anomaly profile generally matching the observed gravity after crustal thinning was applied except for the development of an edge effect anomaly due to the presence of continental necking (marked in red boxes respectively).

With an elevated Moho, the crust that underlies the Dangerous Ground region is thinner than the crust underneath the Sabah onshore region by ~ 10km - ~15km. The thinnest crust (~10km) underlies the NW Sabah Trough, which also has the deepest bathymetry.

5.2.4 A foreland basin model

The resulting structure of the modelled crust and its calculated gravity anomaly after thinning resembles a rifting basin setting, with a thick crust towards onshore and a thinner crust at the basin. Another consequence of crustal thinning is the development of an "edge effect" anomaly (Watts, 2001) on the calculated gravity profile (Figure 5.20). In most rifted margins, this anomaly is commonly associated with the thinning of the crust, resulting "continental necking" at the ocean-continent boundary.

However, based on literature reviews in the study area (Chapter 2), the structure of the NW Sabah margin is probably of a foreland basin setting, where the attenuated crust

of the Dangerous Grounds was subducted and descended beneath the continental margin of Sabah where sediments from the inner margin prograde on to and bury the resulting foreland basin (Sabah Basin).

From seismic interpretations (e.g. Hutchison, 2004), the Sabah Trough was observed to be the onset where the subducting crust starts descending beneath the prograding sediment pile that thickens towards the onshore margin. From this information, the crustal model can be modified to imitate a foreland basin setting (Figure 5.21). This was done by applying a sediment cover that filled the Sabah Basin with lighter density as compared to the crust.

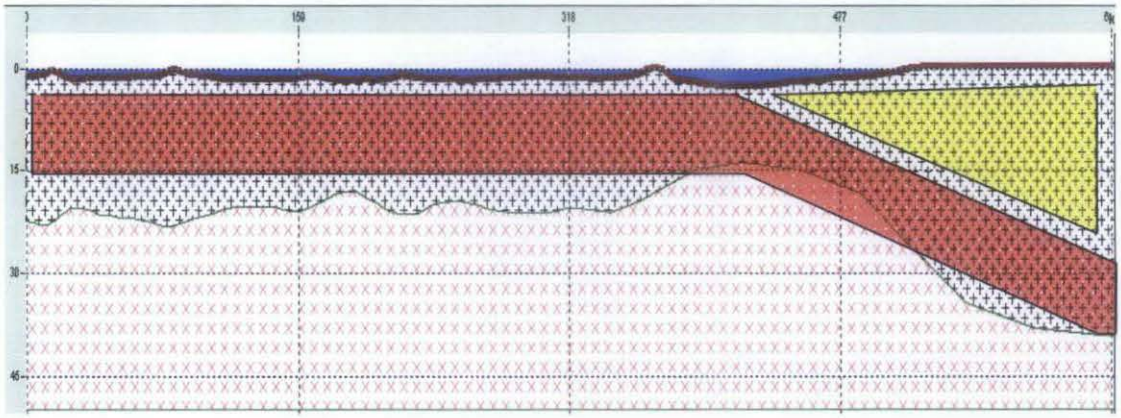

Figure 5.21: Theoretical model resembling a foreland basin setting. The red column represents the subducted Dangerous Grounds crust whereas the yellow column is the prograding sediments that fill the foreland basin (Sabah Basin).

5.2.5 Sediment cover

As described in Chapter 2, the sediments that overlie the crust beneath the Sabah Basin are sediments derived from the uplifted Crocker formation. Mazlan Madon (1999b) also describes the Sabah Basin as a deep foreland basin formed by loading of the continental margin sediments and thrust stacking on an extended continent basement.

The thickness of these sediments were estimated from interpreted seismic profiles (e.g. Hutchison, 2004; Hinz et al., 1989) to be ~2km near the trough and ~12km

towards onshore. The shallower sediments were assumed as 2.3g/cc, whereas the deeper (older and heavier) sediments were assumed as 2.7g/cc, assuming that the basement was made up of thrust sheets from the metamorphosed Crocker formations (Figure 5.22).

These low-density sediments (2.3 g/cc) were needed to suppress the edge effect anomaly. These sediments were interpreted to be Neogene sediments that filled a part of this basin due to progradation of sediments (Mazlan Madon et al., 1999; Hutchison, 2004). In the Sabah Trough, sediment density was assumed to be 2.3 g/cc to simulate low-dense turbiditic sediments which are Upper Miocene to recent age (Hutchison, 2004).

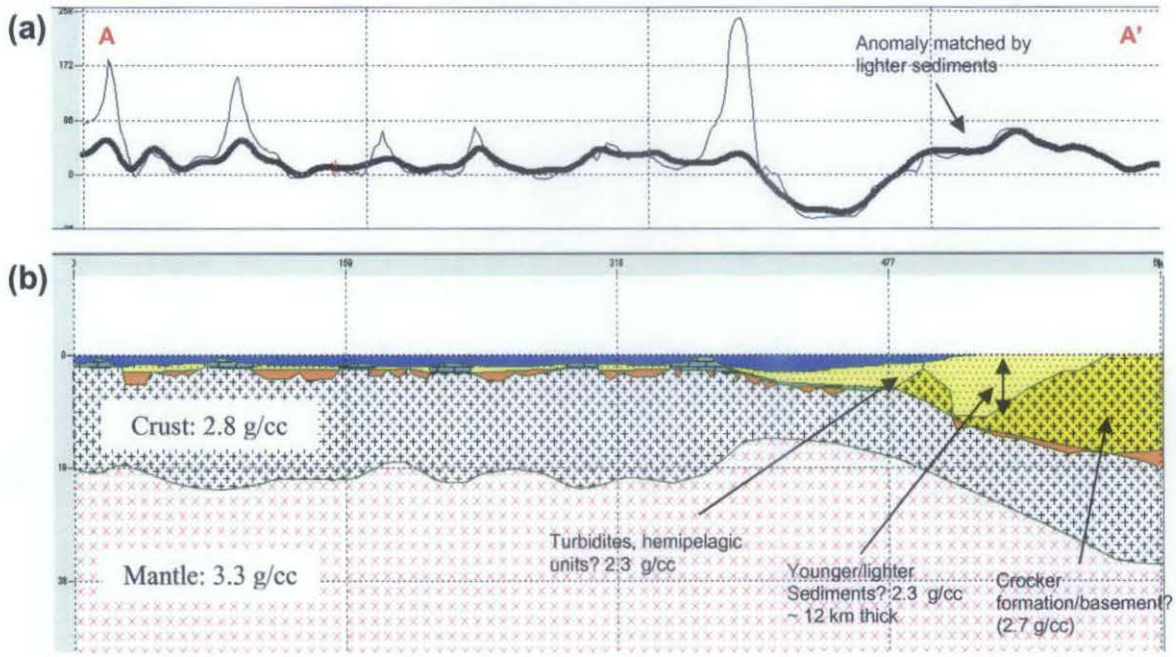

Figure 5.22: a) The gravity anomaly matching over the Sabah Basin with the input of sediments and its respective densities. b) Model resembling a foreland basin setting with sediments.

Over the Dangerous Grounds region, the top of the crust is simulated by syn-rift sediment fill in the form of half grabens. A post-rift sediment layer is draped over the syn-rift sequence. Areas with shallower bathymetry are assumed to be carbonate platforms which also forms the Spratly Islands (Spratly Rise). The high amplitude

gravity anomalies (Figure 5.23 and 5.24) observed over the carbonate platforms were also attenuated by assigning lower densities (~2.2 g/cc).

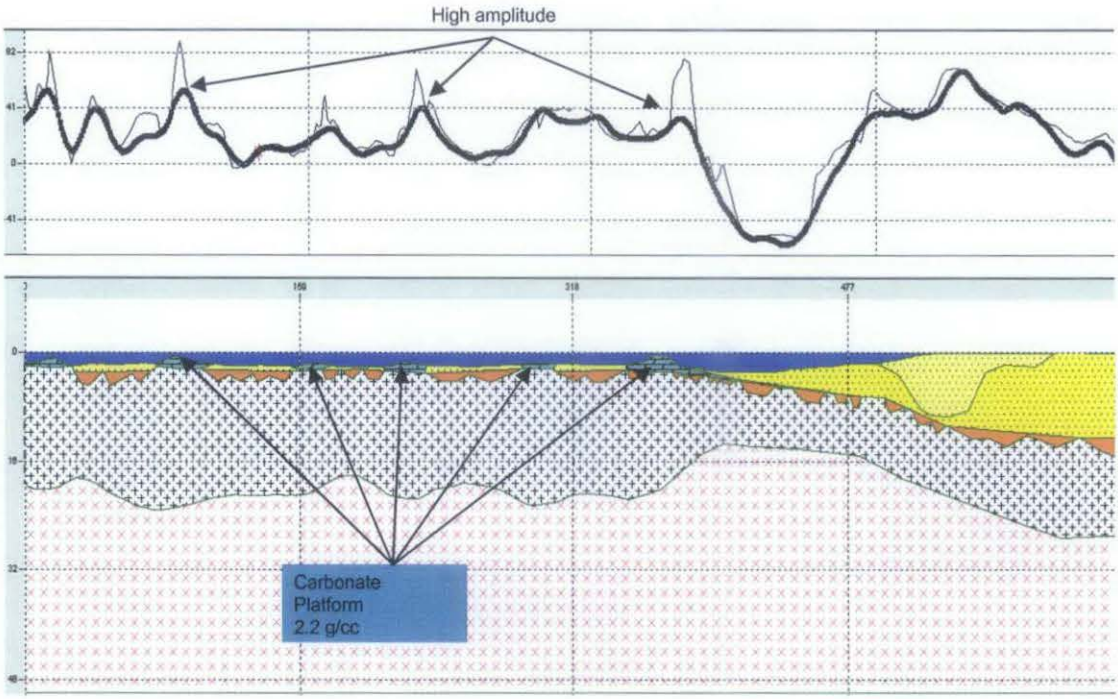

Figure 5.23: Amplitude due to bathymetry highs (carbonate reefs) attenuated using light density carbonate (karstified?) buildups.

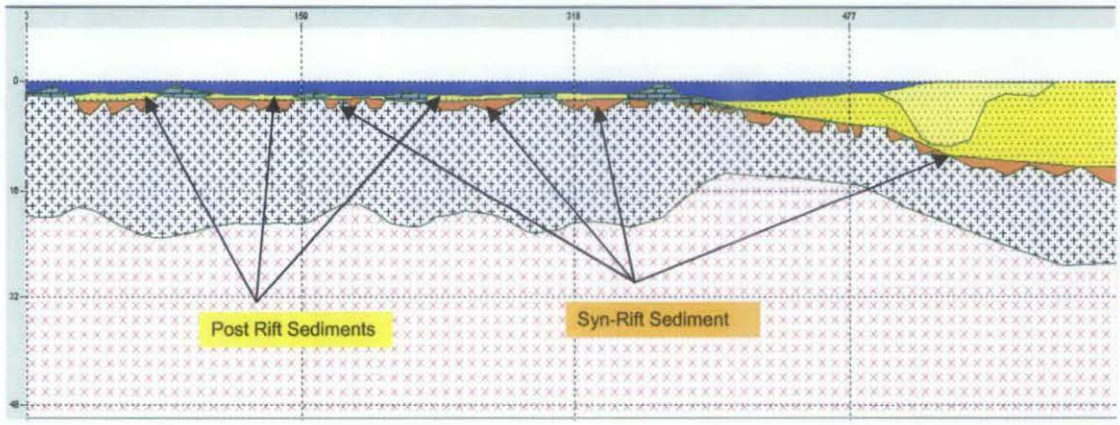

Figure 5.24: Model resembling a foreland basin setting with the input of syn-rift and post-rift sediments.

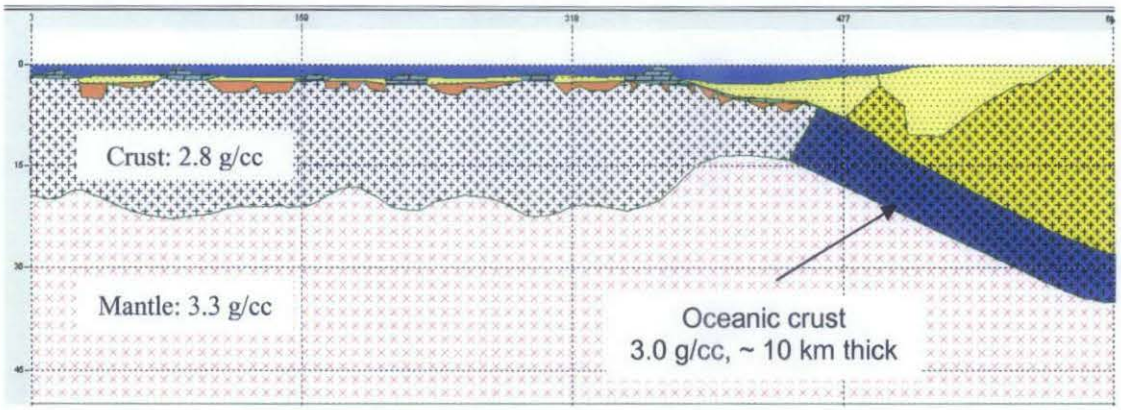

Figure 5.25: Model resembling a foreland basin setting with oceanic crust subducting underneath the Sabah Basin.

5.2.6 Analysis from gravity modelling

In conclusion, an agreement between the observed and calculated gravity anomalies was reached by thinning the crust across the Dangerous Grounds and the Sabah Trough, where the thinnest crust (~10 km) lies beneath the Sabah Trough. Such thinning can be explained by the extensive amount of crustal extension of the Dangerous Grounds since its rifting history occurred during Palaeocene to Eocene.

The thinning of the crust beneath the Sabah Basin could also be explained by having a heavier (3.0 g/cc) subducted oceanic crust (Figure 5.25) that would result in a deeper Moho. However, based on seismic interpretations done previously (Hinz et al. 1989; Hazebroek et al., 1993), the subducting crust is actually the attenuated continental crust.

5.3 Conclusion

GIS provides the capabilities to integrate, visualize and manipulate various datasets for geological studies. For this study, Landsat images, SRTM, bathymetry and satellite derived gravity data were used in a GIS platform to study the basin evolution of NW Borneo. Landsat images and SRTM data provided large data coverage that was suitable for this study. The SRTM data proved to be an excellent source of topographic data, as it's compatibility with the GIS platform and easily acquired.

The application of GIS tools and technologies in the study were used to interpolate and generate hillshade and contour maps that were viewed concurrently with the Landsat images to interpret lineaments. These maps could be viewed in 3D and can open other possibilities for visual analysis. Besides that, profiles of bathymetry and gravity were also extracted from an area of interest to study the lithosphere of the offshore region of NW Borneo.

The majority of lineaments were interpreted as folds from the Rajang-Crocker Fold Thrust Belt evolved from W-E at southwest of Sarawak to NE-SW at the central region onto Sabah and finally ending in an E-W trend at the northern tip of Sabah. Some lineaments were also interpreted in a NW-SE orientation and cross-cutting this major fold trend. These cross-cutting lineaments could mark strike-slip faults. The change in orientation of the fold trends, together with cross-cutting lineaments support the evidence of multiphase tectonic evolution.

The gravity interpretation was generated using the understanding of the subduction theory of NW Sabah, where many workers interpreted a thinned and attenuated continental crust had been subducted underneath Sabah. It was found that the crust underlying the Sabah Trough is the thinnest compared to its adjacent regions i.e. Sabah Basin and Dangerous Grounds. This extreme crustal thinning could be due to the rifting phase of the Dangerous Grounds prior to the collision with NW Sabah.

5.4 Limitations

The following limitations are observed from the project: -

- The resolution of the remote sensing data is within the range of ~15 meters. If a more detailed study was to be performed, higher resolution imagery for example, Quickbird (0.6 cm resolution) image or Ikonos (<1 m resolution) would be suitable (Gupta, 2003). However these images would be more costly as compared to the Landsat images, and would require more storage capacity and computing power to display the data.

- The Landsat images that are affected by clouds and thick vegetation that might affect visualization and interpretation of the images. It was observed that a positive or negative topography could not be differentiated. Therefore, topographical maps (e.g. contour) were needed to compliment the Landsat images for interpretation.

- A lot of storage capacity and computing power are needed to store and display Landsat (1 - 3 gigabytes) images on the GIS. Processing (interpolating) and displaying SRTM data into 3D surface maps (TIN, contour) also require a lot of time and computing power. Without sufficient computing power, the user might experience lags during interpretation.

5.5 Recommendations for future studies

If further studies were to be conducted, the following should be considered: -

- Higher resolution remote sensing images (Ikonos, Quickbird) should be studied to test its application and suitability structural studies. However as mentioned, a lot of computer storage capacity and computing speed would be needed if this were to be attempted.

- ArcGIS's 3D Analyst could be used further more to generate TIN images (Figure 5.27) from the SRTM data for the entire onshore region of the study area. The Landsat image could also be visualized in 3D if it was draped with SRTM derived surface maps (TIN, contour). This could unlock better potential for visual analysis and interpretation to be performed.

- Onshore gravity data could be acquired and integrated into the GIS. Using the same process as in this study, gravity interpretation can be carried out for the onshore region using the SRTM data as topographic input instead. This could be used to extend the understanding of the lithosphere and basin evolution of the onshore region.

Figure 5.26: A TIN image of a portion of the Crocker formation in Sabah generated from the SRTM data.

REFERENCES

Abarca, M.A.A., 2006. Lineament extraction from digital terrain models. Msc Thesis. International Institute for Geo-Information Science and Earth Observation Enschede, Netherlands.

Andersen, O. B., Knudsen, P., 1997. Global gravity field from the ERS-1 and GEOSAT Geodetic Mission Altimetry – The Maditerrenean Sea. From http://www.earth.esa.int/workshops/ers97/papers/andersen2/011c.htm.

Briais, A., Patriat, P., and Tapponnier, P., 1993. Updated interpretation of magnetic anomalies and seafloor spreading stages in the South China Sea: Implications for the Tertiary tectonics of Southeast Asia. Journal of Geophysical Research, 98, 6299-6328.

Benard, F., Muller, C., Letouzey, J., Rangin, C., Tahir, S., 1989. Evidence of multiphase deformation in the Rjang-Crocker range (northern Borneo) from Landsat imagery interpretation: Geodynamic implications.

ESRI, 2006. Arc Gis Desktop Help.

EarthSat, 2004. Geocover Product Description Sheet. From https://zulu.ssc.nasa.gov/mrsid/docs/GeoCover_circa2000_product_description.pdf.

GETECH, 2007. Global Gravity Data. Unpublished GETECH report.

Grant, C.J., 2003. The Pink Fan: A classic deep-marine canyon-fill complex, Block G, NW Sabah. Geological Society of Malaysia Bulletin, 21, 85-94.

Grohmann, C. H., Riccomini, C. and Alves, F. M. 2006. SRTM-based morphotectonic analysis of the Pocos de Caldas Alkaline Massif, southeastern Brazil.

Gupta, R. P., 2003. Remote Sensing Geology, 2nd Edition, Springer-Verlag Berlin Heidelberg, 627pp.

Haile, N.S., 1973. The recognition of former subduction zones in Southeast Asia. In: Tarling, D.H. and Runcorn, S.K., eds. Implications of Continental Drift to the Earth Sciences, 2. Academic Press, London, 885-892.

Hall, R., 1996. Reconstructing Cenozoic SE Asia. In: Hall, R. and Blundell, D.J., eds., Tectonic Evolution of Southeast Asia. Geological Society of London Special Publication, 106, 153-184.

Hamilton, W., 1979. Tectonics of Indonesian region. Vol. 1078. U.S. Geological Survey Professional Paper. 345 p.

Hayes. D.E., Nissen. S. S., 2005. The South China Sea margins: Implications for rifting contrasts. Earth and planetary science letters, 237, 601-616.

Hazebroek, H.P. and Tan, D.N.K., 1993. Tertiary tectonic evolution of the NW Sabah Continental Margin. Bulletin of the Geological Society of Malaysia, Special publication no 33.

Hazebroek, H.P., Tan, D.N.K., and Swinburn, P, 1994. Tertiary evolution of the offshore Sarawak and Sabah Basins, NW Borneo. Abstracts of the American Association of Petroleum Geologist International Conference & Exhibition, Kuala Lumpur, Malaysia, 21-24 August 1994, American Association of Petroleum Geologist Bulletin, 78, 1144-1145.

Holloway, N.H., 1981. The North Palawan Block, Philippines: its relation to Asian mainland and its role in evolution in the South China Sea. Bulletin of Geological Society of Malaysia, 14, 19-58.

Hutchison, C.S., 1996. The 'Rajang accreationary prism' and 'Lupar Line' problem of Borneo. In: Hall, R. and Blundell, D.J., eds., Tectonic Evolution of Southeast Asia. Geological Society of London Special Publication, 106, 247-261.

Hutchison, C.S., 2004. Marginal basin evolution: the southern South China Sea. Marine and Petroleum Geology, 21, 1129-1148.

Hinz, K., Fritsch, J., Kempter, E.H.K., Mohammad, A.M., Meyer, J., Mohamed, D., Vosberg, H., Weber, J. and Benavidez, J. 1989.Thrust tectonics along the northwest continental margin of Sabah, Borneo. Geologische Rundschau, Band 78, Heft 3.

Hinz, K., and Schluter, H. U., 1985. Geology of the dangerous grounds South China Sea, and the continental margin of southwest Palawan: Results of Sonne cruisers S)-23 and SO-27. Energy, 10, 297-315.

James, D.M.D., 1984. Regional geological setting. In: James, D.M.D., ed., "The geology and hydrocarbon resources of Negara Brunei Darussalam". Muzium Brunei, 34-45.

Knudsen, P., and Andersen, O. B., 1997. Improved recovery of the marine gravity field from combining the ERS-1 with the GEOSAT Geodetic Mission Altimetry. From http://earth.esa.int/workshops/ers97/papers/knudsen1.

Koike, K., Nagano, S., Ohmi, M., 1995. Lineament analysis of satellite images using a Segment Tracing Algorithm (STA). Computers and Geosciences 21 (9), 1091–1104.

Mazlan Hj Madon, 1999a. Plate tectonic elements and evolution of Southeast Asia. The petroleum geology and resources of Malaysia. Petroliam Nasional Berhad (Petronas), 61-72.

Mazlan Hj Madon, 1999b. Basin types, tectono-stratigraphic provinces, and structural styles. The petroleum geology and resources of Malaysia. Petroliam Nasional Berhad (Petronas), 79-119.

Mazlan Hj Madon, 1999c. Geological Setting of Sarawak. The petroleum geology and resources of Malaysia. Petroliam Nasional Berhad (Petronas), 275-290.

Mazlan Hj Madon, Leong Khee Meng and Azlina Anuar, 1999. Sabah Basin. The petroleum geology and resources of Malaysia. Petroliam Nasional Berhad (Petronas), 275-290.

Masoud, A., Koike, K., 2006. Tectonic architecture through Landsat -7 ETM+/SRTM SEM-derived lineaments and relationship to hydrogeologic setting in Siwa region, NW Egypt. Journal of African Earth Sciences, 45, 467-477.

Milsom, J., Holt, R., Dzazali bin Ayub and Smail, R., 1997. Gravity anomalies and deep structural controls at the Sabah-Palawan margin, South-China Sea. In: Fraser, A.J., Matthews, S.J. and Murphy, R.W., eds., Petroleum Geology of Southeast Asia. Geological Society of London Special Publication, 126, 417-427.

Nettleton, L. L., 1971. Elementary Gravity and Magnetics for Geologist and Seismologist. In: Wuenschel P.C., ed., Monograph Series Number 1, Society of Exploration Geophysicist, 121pp.

Pubellier, M., Ego, F., Chamot-Rooke, N., Rangin, C., 2003. The building of pericratonic mountain ranges: structural and kinematic constraints applied to GIS-based reconstruction of SE Asia. Bulletin Society Geology of France, n°6, 561-584.

Raharimahefa, T. and Kusky, T.M., 2006. Structural and remote sensing studies of the southern Betsimisaraka Suture, Madagascar. Gondwana Research, 10, 186-197.

Rodriguez, E., C.S. Morris, J.E. Belz, E.C. Chapin, J.M. Martin, W. Daffer, S. Hensley, 2005, An assessment of the SRTM topographic products, Technical Report JPL D-31639, Jet Propulsion Laboratory, Pasadena, California, 143 pp. From http://www2.jpl.nasa.gov/srtm/srtmBibliography.html.

Sandwell D.T. and Smith, W.H.F., 1997. Marine gravity anomaly from Geosat and ERS 1 satellite altimetry. Journal of Geophysical Research, 102, 10,039-10,054.

Sandwell D.T. and Smith, W.H.F., 2006. Exploring the ocean basins with satellite altimeter data. From http://www.ngdc.noaa.gov/mgg/bathymetry/predicted/explore.HTML#intro.

Scherer, F.C., 1980. Exploration in East Malaysia over the past decade. In: Halbouty, M.T. ed., Giant Oil and Gas Fields of the Decade 1968-1978. American Association of Petroleum Geologist Memoir, 30, 423-440.

Schluter, H.U., Hinz, K. and Block, M., 1996. Tectono-stratigraphic terranes and detachment faulting of the South China Sea and Sulu Sea. Marine Geology, 130, 39-78.

Solomon, S., 2003. Remote Sensing and GIS: Applications for Groundwater Potential Assessment in Eritrea. PhD Thesis. Environmental and Natural Resource Information Systems. Royal Institude of Technology, Sweden.

Solomon S. and Ghebreab, W., 2006. Lineament characterization and their tectonic significance using Landsat TM data and field studies in the central highlands of Eritrea. Journal of African Earth Sciences, 46, 371-378.

Taylor, B., and Hayes, D.E., 1980. The tectonic evolution of the South China Basin. In Hayes, D.E., The tectonic and geological evolution of Southeast Asian Seas and Islands. American Geophysical Union, Geophysical Monograph, 23, 89-104.

Taylor, B., and Hayes, D.E., 1983. Origin and the History of the South China Sea Basin. In: The Tectonic and Geological Evolution of Southeast Asian Seas and Islands. (Geophysical Monograph 27) American Geophysical Union, Washington, 23-55.

Tongkul, F., 1999. Regional geological correlation of Paleogene sedimentary rocks between Sabah and Sarawak, Malaysia. In: Geosea 1998 Proceedings, Bulletin of Geological Society Malaysia, 43, 31-39.

Yan, P. and Liu, H., 2004. Tectonic-stratigraphic division and blind fold structures in Nansha Waters, South China Sea. Journal of Asian Earth Sciences 24, 337-348.

Walker, R.T., 2006. A remote sensing study of active folding and faulting in southern Kerman province, S.E. Iran. Journal of Structural Geology, 28, 654-668.

Wang, T.K., Chen, K.C., Lee, C.S., Xia, K., 2006. Seismic imaging of the transitional crust across the northeastern margin of the South China Sea. Tectonophysics, 412, 237-254.

Watts, A.B., Isostasy and Flexure of the Lithosphere, Cambridge University Press, 2001, 506pp.

WEBSITES

- Shuttle Radar Topographic Mission (SRTM) data downloaded from - http://srtm.csi.cgiar.org/SELECTION/inputCoord.asp.

- Landsat Geocover data downloaded from – https://zulu.ssc.nasa.gov/mrsid/